공학박사 학위논문

Low-Complexity Schemes for Class-III and CORR SLM in OFDM Systems

OFDM 시스템에서 Class-III 및 CORR SLM을 위한
저복잡도 방식

2015 년 8 월

서울대학교 대학원

전기컴퓨터공학부

우 준 영

Abstract

Low-Complexity Schemes for Class-III and CORR SLM in OFDM Systems

Jun-Young Woo
Department of EE and CS
The Graduate School
Seoul National University

In this dissertation, orthogonal frequency division multiplexing (OFDM) system is studied. Since OFDM signal sequence undergoes high peak-to-average power ratio (PAPR), several schemes are proposed to mitigate the PAPR problem. PAPR reduction schemes such as selected mapping (SLM) and partial transmit sequence (PTS) are introduced. Due to the high computational complexity of the SLM scheme, low-complexity SLM schemes have been proposed by many researchers. Class-III SLM scheme [55] requires only one inverse fast Fourier transform (IFFT) operation, whereas the conventional scheme needs U IFFT operations. By randomly selecting the cyclic shift and rotation values, this scheme can generate up to N^3 alternative OFDM signal sequences. The PAPR reduction performance of Class-III SLM scheme is little degraded compared to the conventional SLM scheme. Recently, instead of PAPR reduction, the different performance criteria for SLM scheme are proposed such as inter modulation distortion [38] and correlation (CORR) [56]. The objective of these schemes are enhancing the bit error rate (BER) performance instead of PAPR reduction performance.

In the first part of this dissertation, a deterministic selection method of phase se-

quences is proposed for Class-III SLM scheme [55]. First, the optimal condition of cyclic shift values in the Class-III SLM scheme is proposed. Then, the cyclic shift values satisfying the optimal condition is also derived. Compared to the random selection method, the proposed selection method guarantees the optimal PAPR reduction performance. Second, two generation methods for good alternative OFDM signal sequences are proposed, one by using rotation values which do not have linear relation and the other with no rotation values. The advantages of the proposed selection schemes are: (a) The second proposed selection scheme does not need the rotation values. (b) Both of the proposed selection schemes require less side information than random selection scheme. (c) The first proposed selection scheme guarantees the optimal PAPR reduction performance in terms of variance of correlation.

In the second part of this dissertation, the proper oversampling rate for the CORR SLM scheme is proposed. It is known that four times oversampling is enough to estimate the PAPR of the continuous OFDM signal. By calculating the correlation coefficient between the continuous and two times oversampled OFDM signal sequences, it is found that two times oversampling is enough to achieve the same BER performance as four times oversampling case in the CORR SLM scheme. In the simulation results, the same BER performance can be achieved by the proposed two times oversampling rate as four times oversampling case.

Keywords : Bit error rate (BER), correlation (CORR) metric, Orthogonal frequency division multiplexing (OFDM), peak-to-average power ratio (PAPR), selected mapping (SLM)

Student Number : 2011-30965

Contents

List of Tables

List of Figures

Chapter 1. Introduction

1.1. Background

Since the demands of high data rate transmission are increased, multicarrier modulation schemes have been used in wireless communication systems. The main idea of multicarrier modulation is dividing the high-rate data into several low-rate data streams and thus it uses the bandwidth efficiently. Orthogonal frequency division multiplexing (OFDM) [1] is one of the most famous multicarrier modulation technique. Because of the orthogonality of their subcarriers, the receiver can recover the transmitted data without any interferences between two adjacent subcarriers.

OFDM has been adopted as a standard in digital audio broadcasting (DAB) [2] and digital video broadcasting (DVB) [3] in Europe (ETSI DVB-T) and Japan (ARIB ISDB-T). And wireless local area network (WLAN) [4] is adopting OFDM modulation scheme as a standard in Europe (ETSI HIPER-LAN/2), North America (IEEE 802.11a), and Japan (ARIB HiSWANa). This success of OFDM has an impact on being a candidate standard for future wireless communication systems.

It is shown OFDM signal sequence can be generated by using inverse discrete Fourier transform (IDFT) [5]. Later, inverse fast Fourier transform (IFFT) is used instead of IDFT due to the simple implementation of it. Cyclic prefix to avoid inter-symbol inter-

ference (ISI) is proposed [6].

Although OFDM is a charming technique, it has several drawbacks such as high sensitivity to inter-channel interference, I/Q mismatch, and high peak-to-average power ratio (PAPR) in time domain OFDM signals. High PAPR causes significant in-band distortion and out-of-band radiation when it passes through the nonlinear high power amplifier (HPA). Therefore, it is strongly recommended to reduce the PAPR of OFDM signal sequences.

To reduce the PAPR of OFDM time domain signals, several techniques have been researched for many years such as clipping, coding, tone reservation (TR), tone injection (TI), active constellation extension (ACE), selected mapping (SLM), and partial transmit sequence (PTS).

Clipping is the simplest way to reduce the PAPR of OFDM signal sequences. It clipped the magnitude larger than a certain threshold. It reduces the PAPR efficiently, however in-band distortion and out-of-band radiations are generated. Codding scheme uses various known coding methods to reduce the PAPR. It shows good PAPR reduction performance, whereas it causes data rate loss due to the redundancy of coding. TR uses the peak reserved tones (PRT), which only used to reduce the PAPR of OFDM signal sequence. It is known that all one elements for PRT generates low secondary peak of peak reduction signal. Since the PRTs are not used for data tones, TR causes data loss. Generally, 5% of total subcarriers is used for PRT. Recently, TR scheme using clipping noise is proposed. The convergence speed of it is faster than the conventional TR. However, the computational complexity is high due to the iterative FFT and IFFT operations. ACE modifies the constellation to reduce the PAPR. Only the outer-points of constellation are considered, then moved far from the center point. Note that not all

outer-points are moved outside. This extension of constellation causes power increase of transmitted signal. TI also modified the constellation by moving a point to another which are exactly the same position in another constellation. This scheme also increases the power of transmitted signal.

SLM and PTS schemes generate several alternative OFDM signal sequences which have the same information by using the rotation vectors. Among the alternative OFDM signal sequences, the one with the lowest PAPR is selected for transmission. In SLM and PTS schemes, the transmitter should send the side information of which phase sequence is selected in the transmitted OFDM signal. It is known that independent phase sequences are required to achieve good PAPR reduction performance. Since SLM and PTS schemes require multiple IFFT operations, the computation complexity of those schemes are relatively high. Due to this, several low-complexity SLM and PTS schemes have been proposed.

Instead of PAPR reduction of OFDM signals, other schemes such as correlation (CORR) SLM and inter-modulation distortion (IMD) PTS schemes are proposed to enhance the BER performance in the presence of nonlinear HPA. In the CORR SLM scheme, CORR metric is used instead of PAPR metric. CORR calculates the correlation between input and output OFDM signal sequences. Then, an alternative OFDM signal sequence with the maximum CORR value is selected for transmission. Side information about selected phase sequence is transmitted to the receiver. Consequently, better bit error rate (BER) performance can be obtained compared to the conventional SLM scheme using PAPR metric.

1.2. Overview of Dissertation

The rest of this dissertation is organized as follows. OFDM system model and definition of PAPR is introduced in Chapter 2. PAPR reduction schemes and low-complexity SLM schemes are introduced in Chapter 3. Several BER reduction schemes are described in Chapter 4.

In Chapter 5, low-complexity scheme for Class-III SLM scheme is proposed. Class-III SLM scheme uses one IFFT operation instead of U operations for the conventional SLM scheme. Therefore, the computational complexity of Class-III SLM scheme is reduced. Also, N^3 alternative OFDM signal sequences can be generated by using different cyclic and rotation values for each alternative OFDM signal sequence. However, the PAPR reduction performance of that scheme is little degraded compared to the conventional SLM scheme since there are correlations between alternative OFDM signal sequences. In addition to this, the side information of Class-III SLM scheme is very high compared to the conventional SLM scheme. To overcome these shortcomings, a selection method of the optimal cyclic shift values for Class-III SLM scheme is proposed. Also, a selection method of good additional alternative OFDM signal sequences by using proper rotation values is proposed. $N/8$ alternative OFDM signal sequences satisfying the optimal condition by using the optimal cyclic shift values are also proposed. To generate more than $N/8$ alternative OFDM signal sequences, rotation values which do not have linear relation are used. For the proposed scheme, only U pre-determined optimal cyclic shift values are required.

There are some advantages of the proposed scheme. First, the random scheme requires memory for 3 complex numbers (rotation values), whereas the proposed scheme

does not need the memory for rotation values. Second, the random scheme requires $\lceil \log_2 (N/4)^3 \rceil$ bits of side information for cyclic shift values and $\lceil \log_2 4^3 \rceil$ bits of side information for rotation values. Whereas, the proposed scheme requires only $\lceil \log_2 U \rceil$ bits of side information if the cyclic shift values in Table 5.2 are shared by transmitter and receiver. Note that the side information for the proposed scheme is a function of U. Whereas, that of the random scheme is a function of N. Since $N \gg U$, that of the random scheme is much larger than the proposed scheme. Assume that 16-QAM modulation is used. Then, 4 bits (one symbol) of side information is required for the proposed scheme when $N = 1024$ and $U = 16$. Whereas, that of the random scheme is 30 bits (8 symbols). Therefore, the proposed scheme requires much less side information than random scheme. Third, the random scheme has a risk to select the cases of bad PAPR reduction performance, whereas the proposed scheme always guarantees the optimal PAPR reduction performance in terms of minimizing VC.

In Chapter 6, the oversampling effect for the SLM scheme using CORR metric is analyzed in the presence of nonlinear HPA. It is known that four times oversampling is used for CORR SLM scheme. However, it is shown that the BER performance with two times oversampling is the same as four times oversampling case in this dissertation. The oversampled signals for CORR metric computation can be obtained by linear combination of Nyquist-rate samples. By calculating the correlation coefficients of resultant coefficient sequences, it is shown that two and four times oversampling cases show relatively high correlation with 16 times oversampling case. However, Nyquist-rate sampling case shows relatively low correlation with 16 times oversampling case. Also, the probability of choosing the same phase sequence as the 16 times oversampling case is described. Simulation results show that BER performance of two times oversampling

for CORR metric calculation is almost the same as that of four or 16 times oversampling cases. On the other hand, the BER performance for Nyquist-rate sampling case is degraded. Consequently, two times oversampling for CORR metric computation can be used to achieve the same BER performance as those of the four or 16 times oversampling case in the SLM scheme. By using this, the computational complexity for CORR computation can be reduced 33% as that of the four times oversampling case. Also, IFFT size can be reduced to half.

Finally, concluding remarks are given in Chapter 7.

Chapter 2. OFDM System Model

OFDM is based on spreading the data over large number of orthogonal subcarriers that are modulated by low rated data. The spectra of subcarriers in OFDM signals are overlapped where subcarriers are orthogonal to each other. This characteristic of OFDM signal provides better spectral efficiency and eliminates the necessity of steep bandpass filter.

The OFDM scheme offers possibilities of alleviating the drawbacks of single carrier modulation system. It has the advantage of spreading out a frequency selective fading over many symbols because OFDM signal is demodulated symbol by symbol. This makes OFDM more appropriate for high data rate transmission system.

In Section 2.1, OFDM system is described and in Section 2.2, we introduce the orthogonality principle and OFDM modulation. In Section 2.3, we explain fast fourier transform (FFT) algorithm. In Section 2.4, the method for eliminating intersymbol interference (ISI) and interchannel interference (ICI) is described.

2.1. OFDM System

OFDM is to split a high rate data stream into a number of low rate streams that are transmitted simultaneously [7]. The serial data stream is divided into N low rate data

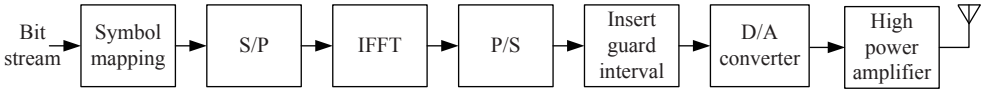

(a)

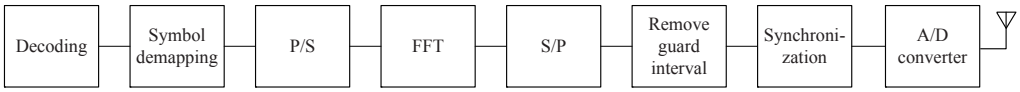

(b)

Figure 2.1: Block diagram of OFDM system: (a) OFDM transmitter and (b) OFDM receiver.

streams, modulated with N subcarriers, and transmitted over the channel. Each data stream is loaded on the subcarrier and then all subcarriers are summed. Thus, the parallel data stream is transformed to serial time domain signal sequence and guard interval is added to avoid ISI. Each subcarrier uses a certain modulation scheme such as phase shift keying (PSK) or M-ary quadrature amplitude modulation (QAM). Loading the data on the subcarriers can be easily implemented by IFFT. All subcarriers can be separated in the receiver because they are orthogonal each other. The output signal of the IFFT is given as

$$x(t) = \frac{1}{\sqrt{N}} \sum_{k=0}^{N-1} X_k e^{j\frac{2\pi k}{T_s}t}, \quad 0 \le t \le T_s \tag{2.1}$$

where X_k is kth element of input symbol sequence $\mathbf{X}$, N is the number of subcarriers, and T_s is symbol duration.

In the OFDM systems, the input symbol sequence is given as $X_0, X_1, X_2, \cdots, X_{N-1}$ with the time duration T_s/N. After splitting the serial data into N parallel data streams, all substreams are multiplied by subcarriers and then they are summed. And we add

guard interval to avoid ISI. In time domain, the discrete OFDM signal sequence is converted to analog OFDM signal before transmitting through the channel. At the receiver, the received OFDM signal is demodulated in the reverse order of transmitter as in Fig. 2.1.

2.2. Modulation and Demodulation of OFDM Signal

2.2.1. Orthogonality Principle

Let $g_k(t)$ be the complex sinusoidal function defined by

$$g_k(t) = \begin{cases} e^{j2\pi f_k t}, & 0 \le t < T_s \\ 0, & \text{otherwise} \end{cases} \tag{2.2}$$

where $f_k = k/T_s$ and k is an integer. And let define

$$\Psi_{n,k}(t) = g_k(t - nT_s) \tag{2.3}$$

where k means kth subcarrier and n means nth symbol, respectively. The complex sinusoidal function satisfies the following relationship

$$\begin{aligned} \frac{1}{T_s}\int_0^{T_s} g_i(t)g_k^*(t)dt &= \frac{1}{T_s}\int_0^{T_s} e^{j2\pi\frac{i}{T_s}t}e^{-j2\pi\frac{k}{T_s}t}dt \\ &= \frac{1}{T_s}\int_0^{T_s} e^{j2\pi\frac{(i-k)}{T_s}t}dt \\ &= \begin{cases} 1, & i = k \\ 0, & \text{otherwise.} \end{cases} \end{aligned} \tag{2.4}$$

Each pair of sinusoidal functions meet the orthogonality if frequency of each sinusoidal is multiple of $1/T_s$. Then, we have $\frac{1}{T_s}\int_0^{T_s} g_i(t)g_k^*(t)dt = \delta(i-k)$, where $\delta(\cdot)$ is

Kronecker delta function. And we also have

$$\int_{-\infty}^{\infty} \Psi_{l,i}(t)\Psi^*_{m,j}(t)dt = \delta(l-m)\delta(i-j). \tag{2.5}$$

If we use multiple of symbol frequency $f_k = k/T_s$ as a subcarrier of the OFDM signal, all of subcarriers are orthogonal. It is clear that the OFDM signal sequences can be easily demodulated.

2.2.2. OFDM Signal Modulation and Demodulation

The baseband OFDM signal sequence is modulated with N subcarriers. The baseband OFDM signal x_t is given as

$$x_t = \sum_{n=-\infty}^{\infty} \sum_{k=0}^{N-1} X_{n,k}\Psi_{n,k}(t) \tag{2.6}$$

where $X_{n,k}$ is data loaded on kth subcarrier of nth symbol and $\Psi_{n,k}(t)$ is defined in (2.3).

The received OFDM signal sequence is demodulated with several integrators and oscillators. Demodulation process can be written as

$$\begin{aligned}
\hat{X}_{n,k} &= \frac{1}{T_s}\int_0^{T_s} x_t\Psi^*_{n,k}(t)dt \\
&= \frac{1}{T_s}\int_0^{T_s} \left(\sum_{i=-\infty}^{+\infty}\sum_{k'=0}^{N-1} X_{i,k}\cdot\Psi_{i,k'}(t)\right)\Psi^*_{n,k}(t)dt \\
&= \frac{1}{T_s}\sum_{i=-\infty}^{+\infty}\sum_{k'=0}^{N-1} X_{n,k'}\int_0^{T_s}\Psi_{i,k'}(t)\Psi^*_{n,k}(t)dt \\
&= \frac{1}{T_s}\sum_{i=-\infty}^{+\infty}\sum_{k'=0}^{N-1} X_{n,k'}\int_0^{T_s}\delta(i-n)\delta(k^{'}-k)dt \\
&= \frac{1}{T_s}X_{n,k}T_s = X_{n,k}.
\end{aligned} \tag{2.7}$$

Using the orthogonality of subcarriers, the received OFDM signal sequence can be easily demodulated when spectra of subcarriers are overlapped.

2.3. Fast Fourier Transform

In the past, it was very difficult to implement an OFDM modulation system because OFDM signal sequence is composed of many subcarriers. Although OFDM is an effective modulation method to use bandwidth efficiently, it should have the same modulators as the number of subcarriers. It may be very burdensome to make modulators for all subcarriers. But, it is possible to reduce the number of modulators and demodulators by using IFFT and FFT, respectively, which were proposed by Weinstein [5].

The OFDM signal sequence is the sum of data bearing sinusoidals whose frequencies are multiple of $1/T_s$. Equation (2.1) is equivalent to IFFT given by

$$x_n = \frac{1}{\sqrt{N}} \sum_{k=0}^{N-1} X_k W_N^{-kn}, \;\; k = 0,\; 1, \cdots,\; N-1 \tag{2.8}$$

where $W_N = e^{-j2\pi/N}$ [8]. Thus, IFFT is used in the OFDM systems as a modulator and FFT as a demodulator.

2.4. Guard Interval

In order to generate the OFDM signal, the high rate input symbols are divided into N parallel low rate input symbols. Thus, each input symbol duration becomes N times longer and delay spread in the multipath fading channel can be ignored. If there are no ISI and ICI [9], [10], individual subcarrier in the OFDM signal can be completely sepa-

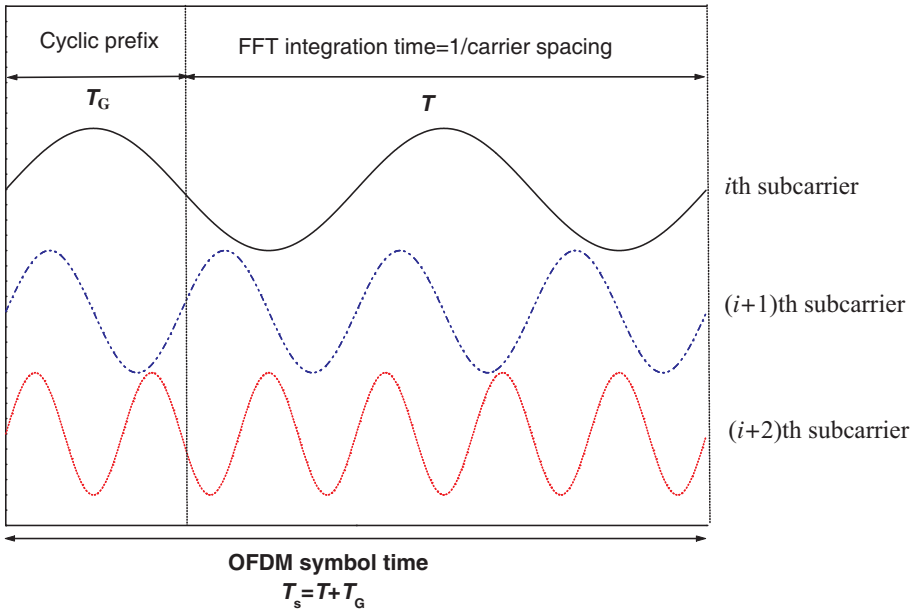

Figure 2.2: OFDM symbol with cyclic extension.

rated by FFT at the receiver. When distortions occur among subcarriers by delay spread, it seems to cause ISI. To eliminate the ISI in the OFDM signals, the guard interval is inserted between OFDM signals. And this is done by making the guard interval duration larger than that of the delay spread in the channel [5].

In the early days, the guard interval is left empty. But if the guard interval is empty, the orthogonality among subcarriers can be destroyed which causes ICI. In order to eliminate ISI as well as ICI, the OFDM symbol should be cyclically extended into the guard interval [6]. This preserves the orthogonality among the delayed subcarriers by satisfying the orthogonal principle. Thus, we can eliminate ISI and ICI by the guard interval and making the guard interval duration longer than the delay spread. Fig. 2.2 shows OFDM symbol time and its cyclic prefix filled with extension of OFDM symbol.

2.5. Peak-to-Average Power Ratio

OFDM is an attractive scheme in the multipath fading channel but the OFDM signal has a critical drawback that it has high PAPR. This causes the distortion of the OFDM signal, because the signals with high PAPR require wide linear range of nonlinear HPA compared to that with lower PAPR and it also increases the BER. In this chapter, we introduce PAPR and its probabilistic distribution in the OFDM signal sequence.

2.5.1. Definition

In the OFDM system, the OFDM signal sequence is generated by summing sinusoidal signals. And each sinusoidal signal corresponds to the subcarrier. Therefore the OFDM system using a lot of subcarriers has to sum the sinusoidal signals which make high PAPR. The PAPR, as a measurement of a waveform, is defined as

$$\mathrm{PAPR}(x_n) = \frac{\max\limits_{0 \le n \le N-1} |x_n|^2}{E[|x_n|^2]} \tag{2.9}$$

where $E[\cdot]$ denotes the expectation.

2.5.2. The distribution of PAPR

The complementary cumulative distribution function (CCDF) is widely used for measuring the PAPR reduction performance. The CCDF of the PAPR denotes the probability that the PAPR of an OFDM signal sequence exceeds a given threshold value. From the central limit theorem, the CCDF of the real and imaginary parts of the OFDM signal sequence can be approximated as Gaussian distribution [11]. This approximation is more accurate for the cases of large number of subcarriers. Thus the amplitude of multicarrier

signal has Rayleigh distribution, that is,

$$f_u(u) = \frac{2u}{\sigma^2} \exp\left(- \frac{u^2}{\sigma^2} \right), \quad u > 0 \tag{2.10}$$

where σ^2 denotes the variance of OFDM signal sequence.

Then, the probability that the magnitude of an OFDM signal sequence does not exceed a certain threshold level x_0 can be calculated as

$$\begin{aligned} \Pr\{|x_n| < x_0\} &= \int_0^{x_0} f_u(u) du \\ &= 1 - \exp\left(- \frac{x_0^2}{\sigma^2} \right). \end{aligned} \tag{2.11}$$

Now, assume that $x_n,\ 0 \le n \le N-1$ be statistically independent [12]. Then, the probability that at least one subcarrier is larger than certain threshold level x_0 is given as

$$\begin{aligned} \Pr\{\exists n \text{ s.t. } |x_n| > x_0,\ 0 \le n \le N-1\} &= 1 - \Pr\left\{ \max_{0 \le n \le N-1} |x_n| < x_0 \right\} \\ &= 1 - \left(\Pr\left\{ |x_n| < x_0 \right\} \right)^N \\ &= 1 - \left(1 - \exp\left(- \frac{x_0^2}{\sigma^2} \right) \right)^N \end{aligned} \tag{2.12}$$

Let $\gamma = x_0^2/\sigma^2$. Müller and Huber in 1997 [12] calculated CCDF by using (2.11). The probability that at least one magnitude of the OFDM signal samples exceeds a certain threshold γ can be approximated as

$$\Pr\{\text{PAPR} > \gamma\} = 1 - \left(1 - \exp(-\gamma) \right)^N. \tag{2.13}$$

2.5.3. PAPR of Oversampled Signal

Oversampling can be easily implemented by zero padding to the input symbol sequence. Zero padded input symbol sequence is given as

$$\mathbf{X}_L = [X_0, \cdots, X_{N/2-1}, \underbrace{0, \cdots, 0}_{(L-1)N\ 0's}, X_{N/2}, \cdots, X_{N-1}]. \tag{2.14}$$

L times oversampled OFDM signal sequence can be expressed

$$x_L[n] = \frac{1}{\sqrt{LN}} \sum_{k=0}^{LN-1} X_k e^{j\frac{2\pi nk}{LN}}, \ \ 0 \le n \le LN-1. \tag{2.15}$$

Oversampled signal can be expressed by linear combination of Nyquist-rate samples [16]. The oversampling operator is called interpolator and the impulse response of an interpolator for L times oversampling is defined as

$$h_L[n] = \frac{\sin(\pi n/L)}{\pi n/L}. \tag{2.16}$$

Since an ideal interpolator cannot be implemented, a finite-length filter of length I is used for it in practice. Then, the output of finite-length interpolator can be expressed as

$$\tilde{x}_L[n_L] = \sum_{k=\lceil (n_L-LI)/L \rceil}^{\lfloor (n_L+LI)/L \rfloor} x[k] h_L[n_L - Lk] \tag{2.17}$$

where $\tilde{x}_L[n_L]$ is the estimated n_Lth element of L times oversampled OFDM signal sequence and $x[k]$ denotes the kth element of Nyquist-rate OFDM signal sequence.

Let $x_L[n]$ be nth element of L times oversampled OFDM signal sequence. Then, the PAPR of L times oversampled OFDM signal sequence can be represented as

$$\text{PAPR} = \frac{\max\limits_{0 \le n \le LN-1} |x_L[n]|^2}{E[|x_L[n]|^2]} \tag{2.18}$$

where L denotes the oversampling factor. It is known that four times ($L = 4$) oversampling is enough to estimate the PAPR of continuous OFDM signal [17]. In [18], it is known that true PAPR is at most $1/\cos(\pi/2L)$ times larger than the estimated PAPR when L times oversampling is used and a better estimation when $L = 3/2$ was given in [19].

Chapter 3. PAPR Reduction Schemes

As the OFDM scheme becomes popular, its high PAPR is considered as one of the major drawbacks. The high PAPR of OFDM signal reduces efficiency of the nonlinear HPA and it causes in-band distortion and out-of-band radiation. To overcome this, many PAPR reduction schemes have been proposed. The OFDM also has its performance criteria such as PAPR reduction performance, BER performance, side information [20], and computational complexity. Several PAPR reduction schemes are overviewed in [21] and [22]. In this chapter, the existing PAPR reduction schemes are introduced.

3.1. Clipping

Clipping is the simplest scheme for PAPR reduction of the OFDM signal. Clipping the OFDM signal simply cuts off the magnitude of the time domain OFDM signal to a certain threshold level. If the amplitude of the OFDM signal is lower than a certain threshold value, it passes through the clipper. Otherwise, its magnitude sets to the threshold value, that is,

$$\mathrm{clip}_A(x_k) = \begin{cases} x_k, & |x_k| \leq A \\ A\frac{x_k}{|x_k|}, & |x_k| > A. \end{cases} \tag{3.1}$$

Since this method cuts off the OFDM signal in the time domain without any con-

siderations in the frequency domain, distortion of OFDM signal occurs. The signal distortion causes in-band distortion and out-of-band radiation. In-band distortion results in the degradation of symbol error rate while the out-of-band radiation reduces the efficiency of bandwidth usage. Thus the filtering after clipping is required to reduce the out-of-band radiation. But this may also cause some peak regrowth so that the peak of signal may exceed a certain threshold value of clipping process. To reduce it, a repeated clipping-and-filtering operations can be used [23], [24] in OFDM systems, which results in large amount of computational complexity. Generally, the repeated clipping-and-filtering scheme [23] is used with other PAPR reduction schemes described in the following sections.

3.2. Tone Reservation

TR scheme is proposed by Tellado and Cioffi [25]. The main idea of this method is adding the peak reduction sequence **c** to the OFDM signal x in time domain to reduce the peak of OFDM signal. The peak reduction sequence can be constructed by peak reduction tones (PRT), that is, $\{i_1, i_2, \cdots, i_R\}$.

Let **C** be a peak reduction vector in frequency domain such that $\mathbf{c} = \mathbf{QC}$, where **Q** denotes IFFT matrix. Since **c** is added to **X**, the new time domain signal vector is given as

$$\mathbf{x} + \mathbf{c} = \mathbf{Q}(\mathbf{X} + \mathbf{C}). \tag{3.2}$$

Then the modified PAPR can be defined as

$$\text{PAPR}(\mathbf{x} + \mathbf{c}) = \frac{||\mathbf{x} + \mathbf{c}||_\infty^2}{E\{||\mathbf{x}||_2^2\}} \tag{3.3}$$

where $||\cdot||_s$ denotes the s norm. The TR scheme restricts the input symbol sequence

$\mathbf{X}$ and the peak reduction vector $\mathbf{C}$ to lie in disjoint frequency subcarriers, i.e., $X_k = 0, k \in \{i_1, \cdots, i_R\}$ and $C_k = 0, k \notin \{i_1, \cdots, i_R\}$. This formulation is distortionless and leads to very simple decoding of the data symbols which are extracted from the received sequence by choosing the set of values $k \notin \{i_1, \cdots, i_R\}$ at the receiver. In addition, it allows to adapt simple optimization techniques for the computation of the peak reduction sequence $\mathbf{c}$.

With the peak reduction vector $\mathbf{C}$, the PAPR of the modified OFDM signal sequence $\mathbf{x} + \mathbf{c}$ can be made lower than the PAPR of $\mathbf{x}$. The peak reduction sequence $\mathbf{c}$ that minimizes the maximum peak value should be computed as

$$\min_{\mathbf{c}} ||\mathbf{x} + \mathbf{c}||_\infty = \min_{\hat{\mathbf{C}}} ||\mathbf{x} + \hat{\mathbf{Q}}\hat{\mathbf{C}}||_\infty. \tag{3.4}$$

This optimization method to find the optimal peak reduction sequence $\mathbf{c}$ can be considered as convex on the variables C_n in $\mathbf{C}$ and can be easily computed as the linear programming (LP) method [26]. To reduce the computational complexity of LP, a simple gradient algorithm is proposed in [27].

3.3. Partial Transmit Sequence

The main idea of the PTS scheme [12], [28] is that an input symbol sequence $\mathbf{X}$ is partitioned into V disjoint input symbol subsequences, i.e., $\mathbf{X}_v = [X_{v,0}, X_{v,1}, \cdots, X_{v,N-1}]$, $v = 1, 2, \cdots, V$ such that

$$\mathbf{X} = \sum_{v=1}^{V} \mathbf{X}_v. \tag{3.5}$$

Each subcarrier in the input symbol sequence $\mathbf{X}$ can only belong to one subblock $\mathbf{X}_v$. Then, each input symbol subsequence is multiplied by rotating factor b_v with $|b_v| = 1$

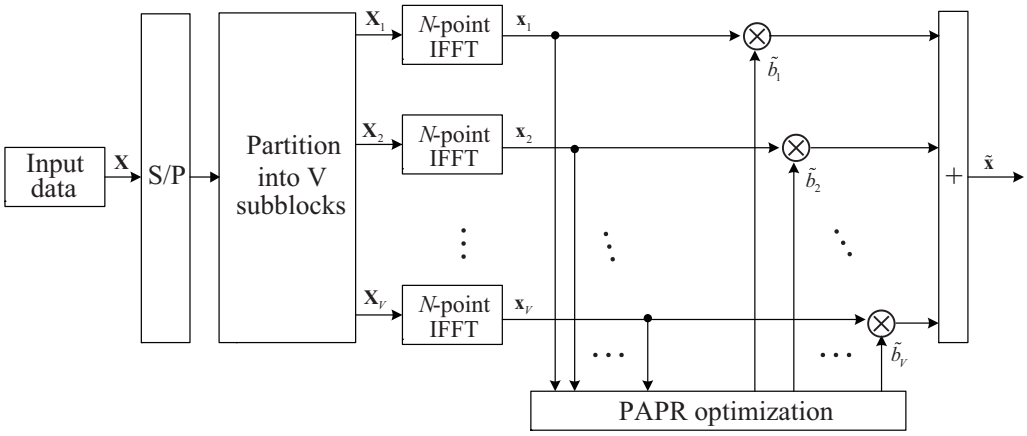

Figure 3.1: Block diagram of PTS scheme.

and they are summed as

$$\hat{\mathbf{X}} = \sum_{v=1}^{V} b_v \mathbf{X}_v. \tag{3.6}$$

Due to the linearity of the IFFT, the V input symbol subsequences are transformed separately and then summed. This process is given as

$$\begin{aligned} \hat{\mathbf{x}} &= \text{IFFT}\left\{ \sum_{v=1}^{V} b_v \mathbf{X}_v \right\} \\ &= \sum_{v=1}^{V} b_v \text{IFFT}\left\{ \mathbf{X}_v \right\} \\ &= \sum_{v=1}^{V} b_v \mathbf{x}_v \end{aligned} \tag{3.7}$$

where $\mathbf{x}_v = \text{IFFT}\{\mathbf{X}_v\}$.

An optimized rotating vector $\tilde{\mathbf{b}} = \left[\tilde{b}_1, \cdots, \tilde{b}_V\right]$ for the minimum PAPR should be chosen as

$$\tilde{\mathbf{b}} = \left[\tilde{b}_1, \cdots, \tilde{b}_V\right] = \underset{[b_1, \cdots, b_V]}{\text{argmin}} \left(\max_{0 \le n \le N-1} \left| \sum_{v=1}^{V} b_v x_{v,n} \right| \right). \tag{3.8}$$

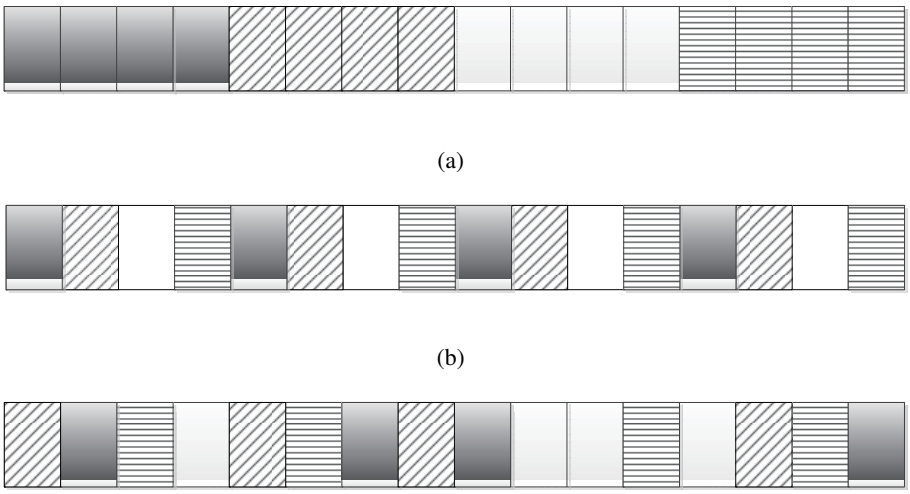

Figure 3.2: Examples of partitioning method in PTS scheme when $N = 16$: (a) Adjacent, (b) interleaved, and (c) random partition.

Therefore, the OFDM signal sequence for transmission is given as

$$\tilde{\mathbf{x}} = \sum_{v=1}^{V} \tilde{b}_v \mathbf{x}_v. \tag{3.9}$$

In the PTS scheme, the transmitter should send the side information of rotating vector $\tilde{\mathbf{b}}$ to the receiver to recover the original symbol sequence.

The PAPR reduction performance depends on the method of subblock partitioning. There exist several subblock partitioning methods such as adjacent, interleaved, and random partitionings. Among them the random partitioning method has the best PAPR reduction performance. However, the computational complexity also slightly increases in the random partitioning method. Thus, there is a trade-off between PAPR reduction performance and the computational complexity.

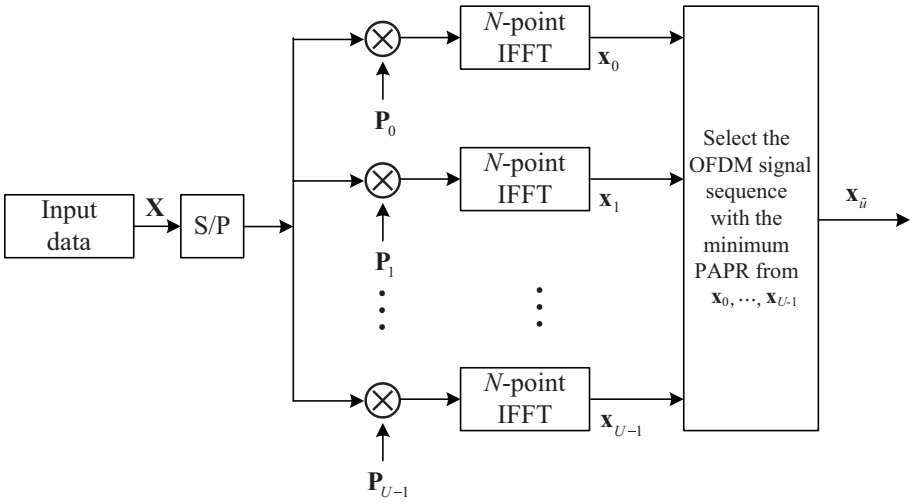

Figure 3.3: Block diagram of SLM scheme.

3.4. Selected Mapping

In the SLM scheme, the input symbol sequences are rotated by phase sequences to generate alternative symbol sequences. Each of these alternative symbol sequences is IFFTed to generate alternative OFDM signal sequences and the one with the lowest PAPR is selected for transmission. A block diagram of the SLM scheme is shown in Fig. 3.3. To generate U alternative symbol sequences that include the same information, each input symbol sequence is multiplied by U different phase sequences, $\mathbf{P}_u$ = $[P_{u,0}, P_{u,1}, \cdots, P_{u,N-1}]$, where $\mathbf{P}_{u,n} = e^{j\phi_{u,n}}$, $\phi_{u,n} \in [0,\ 2\pi)$, $0 \leq n \leq N-1, 0 \leq u \leq U-1$. To represent the original OFDM symbol sequence, usually the first phase sequence $\mathbf{P}_0$ is set to the all-1 sequence vector, i.e., $\mathbf{P}_0 = [1, 1, \cdots, 1]$. Then, U alternative symbol sequences $\mathbf{X}_u = [X_{u,0}, X_{u,1}, \cdots, X_{u,N-1}], 0 \leq u \leq U-1$, are generated, where $\mathbf{X}_u = \mathbf{X} \otimes \mathbf{P}_u$ to represent the component-wise multiplication in Fig. 3.3. Therefore,

alternative OFDM signal sequence can be represented as

$$x_n^u = \frac{1}{\sqrt{N}} \sum_{k=0}^{N-1} X_k P_{u,k} e^{j2\pi \frac{k}{N} n}, \quad 0 \leq n \leq N-1. \tag{3.10}$$

Among U different alternative signal sequences, the one with the lowest PAPR is selected for transmission.

In [12], the following CCDF expression for the OFDM signal sequence with SLM scheme is given as

$$\Pr(\text{PAPR} > \gamma) = (1 - (1 - e^{-\gamma})^N)^U. \tag{3.11}$$

But, in the case of small N, $x_{u,n}$ is not approximately complex Gaussian distributed and thus, each alternative OFDM signal sequence is mutually dependent [12]. Therefore, the CCDF expression (3.11) cannot be used to the OFDM signal sequence with SLM in general.

Information for the selected phase sequence should be transmitted to the receiver as side information. At the receiver, the reverse order operations are performed to recover the input symbol sequence. For implementing the SLM scheme, we needs U IFFT operations and the number of required side information bits are $\lceil \log_2 U \rceil$ for each OFDM symbol, but necessity of side information of SLM scheme causes slight degradation in bandwidth efficiency.

Also, the optimal condition of phase sequences in SLM scheme is proposed in [13] and [14]. However, it is possible that there are correlations between phase sequences. For this case, a criterion for good PAPR reduction performance is proposed in [15].

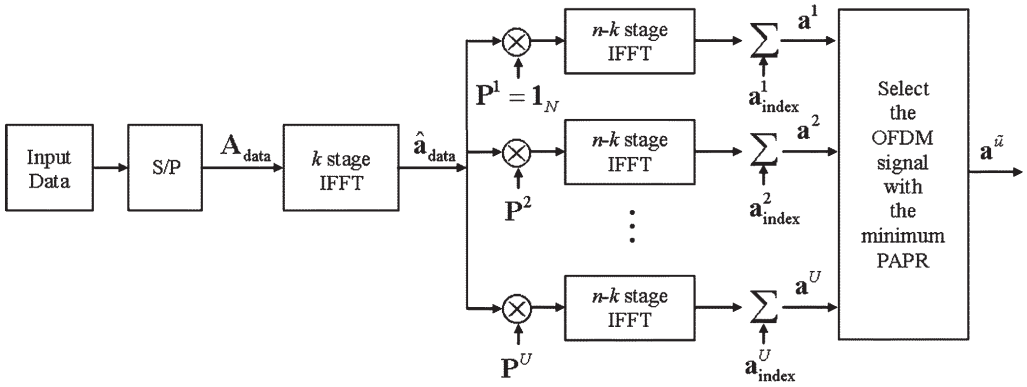

Figure 3.4: A block diagram of SLM scheme with divided IFFT stages [29].

3.5. Low-Complexity SLM Schemes

SLM scheme shows good PAPR reduction performance. However, the computational complexity depends on the number of alternative OFDM signal sequences. If we want to generate more alternative OFDM signal sequences, the more IFFT operations are needed. That is, there is a trade-off between PAPR reduction performance and computational complexity. Since the conventional SLM scheme requires high computational complexity, many low-complexity SLM schemes are proposed. In this section, some low-complexity SLM schemes are introduced.

3.5.1. SLM Scheme with Divided IFFT Stages

For 2^n-point IFFT operation, n stages are required to compute whole IFFT operation. In [29], the stages of IFFT are divided into two steps. First, k stages of IFFT are performed. This intermediate OFDM signal sequence is denoted by $\hat{\mathbf{a}}_{\text{data}}$. Then, uth phase

sequence $\mathbf{P}^{(u)}$ is multiplied to $\hat{\mathbf{a}}_{\text{data}}$ to generate uth alternative OFDM signal sequence as follows.

$$\mathbf{a}^u = \text{IFFT}_{k+1}^n\{\mathbf{P}^{(u)} \otimes \hat{\mathbf{a}}_{\text{data}}\} + \mathbf{a}_{\text{index}}^{(u)} \tag{3.12}$$

where IFFT_j^i denotes IFFT operation from j to i stages and $\mathbf{a}_{\text{index}}^{(u)}$ is uth side information denoted by $\mathbf{A}_{\text{index}}^{(u)}$. The uth side information $\mathbf{a}_{\text{index}}^{(u)}$ is added and should be transmitted to the receiver. Intermediate OFDM signal sequence is used to generate alternative OFDM signal sequences and thus, the computational complexity can be reduced.

3.5.2. Modified SLM Scheme

In the conventional SLM scheme, large number of alternative OFDM signal sequences should be generated to achieve good PAPR reduction performance. In [30], a low-complexity SLM scheme is proposed.

Unlike the conventional SLM scheme, modified SLM scheme uses the first U alternative OFDM signal sequences to generate more alternative OFDM signal sequences. The generation method is expressed as follows.

$$\begin{aligned}\mathbf{a}_u &= \frac{1}{\sqrt{2}}\text{IFFT}\{\mathbf{A}^{\text{data}} \otimes \mathbf{P}_i + j\frac{b}{\sqrt{2}}\text{IFFT}\{\mathbf{A}^{\text{data}} \otimes \mathbf{P}_k\} \\ &= \frac{1}{\sqrt{2}}(\mathbf{a}_i^{\text{data}} + jb\mathbf{a}_k^{\text{data}})\end{aligned} \tag{3.13}$$

where $b \in \{1, -1\}$ and $1 \leq i < k \leq U$. By this method, the modified SLM scheme can generate U^2 alternative OFDM signal sequences. Also, compared to the conventional SLM scheme with the same number of alternative OFDM signal sequences, computation complexity of the modified SLM scheme is reduced up to 60%.

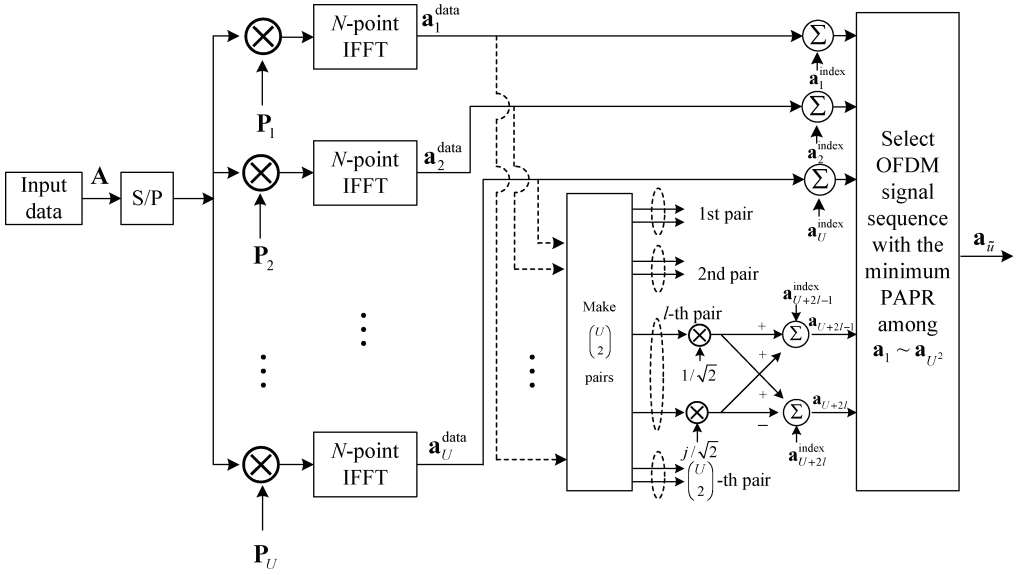

Figure 3.5: A block diagram of modified SLM scheme [30].

3.5.3. SLM Scheme with Conversion Matrices

A SLM scheme with conversion matrices was proposed [31]. The main idea of [31] is shown in Fig. 3.6. OFDM signal sequence $\mathbf{s}$ is generated by IFFT of input symbol sequence $\mathbf{X}$, i.e., $\mathbf{s} = \mathrm{IFFT}\{\mathbf{X}\}$. Then, rth alternative OFDM signal sequence is generated by IFFT of rth alternative symbol sequence $\mathbf{S}_r = \mathbf{R}_r\mathbf{X}$, i.e., $\mathbf{s}_r = \mathrm{IFFT}\{\mathbf{S}_r\}$, where $\mathbf{R}_r$ is the rth phase matrix is given as

$$\mathbf{R}_r = \begin{bmatrix} b_0^{(r)} & & & 0 \\ & b_1^{(r)} & & \\ & & \ddots & \\ 0 & & & b_{N-1}^{(r)} \end{bmatrix}, \quad b_n^{(r)} = \{\pm 1, \pm j\}. \tag{3.14}$$

It is well known that component-wise multiplication in frequency domain becomes

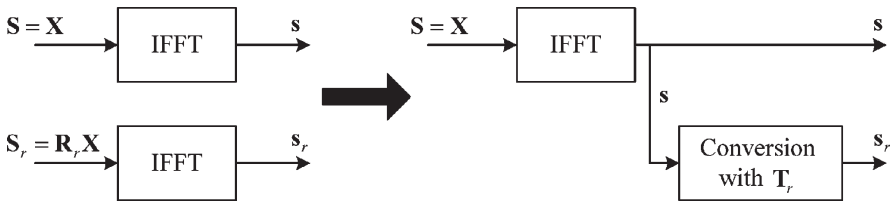

Figure 3.6: The idea of SLM scheme with conversion matrix [31].

convolution in time domain. That study used this simple property of FFT. That is,

$$\begin{aligned}\mathbf{s}_r &= \mathrm{IFFT}\{\mathbf{S}_r\} = \mathrm{IFFT}\{\mathbf{R}_r\mathbf{X}\} \\ &= \mathrm{IFFT}\{\mathbf{R}_r\} \otimes \mathrm{IFFT}\{\mathbf{X}\} \\ &= \mathbf{T}_r \otimes \mathbf{s} \end{aligned} \tag{3.15}$$

where $\otimes$ denotes the circular convolution operator and

$$\mathbf{T}_r = [\mathbf{t}_r, \mathbf{t}_r^{<1>}, \mathbf{t}_r^{<2>}, \cdots, \mathbf{t}_r^{<N-1>}] \tag{3.16}$$

where $\mathbf{t}_r$ is the column vector of $\mathbf{T}_r$ and $\mathbf{t}_r^{<i>}$ is down shifted version of $\mathbf{t}_r$ by i.

Then, authors in [31] found eight types of $\mathbf{T}_r$'s having few nonzero values, which leads to low computational complexity. The condition for finding $\mathbf{T}_r$'s are: (1) The number of nonzero values in a column of $\mathbf{T}_r$ must be 4 and (2) each of nonzero values belongs to $\{\pm 1, \pm j\}$. In Table 3.1, there are eight types of the proposed column vectors $\mathbf{t}_r$'s which have 4 nonzero values.

Consequently, the computational complexity of the SLM scheme in [31] can be reduced compared to the conventional SLM scheme.

Table 3.1: Eight types of the proposed $\mathbf{t}_r$'s with period 4.

$\mathbf{t}_1 = [1, 1, 1, -1]^T$
$\mathbf{t}_2 = [1, 1, -1, 1]^T$
$\mathbf{t}_3 = [1, -1, 1, 1]^T$
$\mathbf{t}_4 = [1, -1, -1, -1]^T$
$\mathbf{t}_5 = [1, j, 1, -j]^T$
$\mathbf{t}_6 = [1, j, -1, j]^T$
$\mathbf{t}_7 = [1, -j, 1, j]^T$
$\mathbf{t}_8 = [1, -j, -1, -j]^T$

3.6. Considerations for PAPR Reduction Schemes

There are several performance criteria for PAPR reduction schemes of OFDM systems such as BER, PAPR reduction performance, and side information. Table 3.2 shows the comparison of various PAPR reduction schemes. SLM scheme shows no BER and power increase, while the computational complexity of SLM scheme is relatively high.

As shown in Table 3.2, there are some trade-offs between criteria for PAPR reduction schemes. While the SLM scheme shows good PAPR reduction performance, its computational complexity is high. Therefore, many studies have been done to lower the computational complexity of the SLM scheme [32], [33]. Also, the computational complexity of zero padded SLM scheme is described in [34].

Table 3.2: Comparison of various PAPR reduction schemes.

Method	BER increase	Data rate loss	Complexity	Power increase
Clipping	Yes	No	Low	No
SLM	No	Low	High	No
PTS	No	Low	High	No
TR	No	Middle	Middle	Yes
ACE [35]	No	No	High	Yes

Chapter 4. BER Reduction Schemes

PAPR has been an interesting research topic of OFDM systems for last 20 years. However, the peak magnitude of OFDM signal sequence can be reduced by the PAPR reduction schemes. The remaining samples of OFDM signal sequence such as secondary peak was not considered. In that sense, PAPR reduction schemes are non-optimal in terms of BER performance of OFDM systems. Therefore, another metric is proposed to enhance BER performance of OFDM systems. In this chapter, some BER reduction schemes of OFDM systems with nonlinear HPA are introduced. Note that the proposed BER reduction schemes can be used instead of PAPR reduction schemes.

4.1. PTS Scheme with PICR Metric

The complex baseband OFDM signal is expressed as [36]

$$x(t) = \frac{1}{\sqrt{N}} \sum_{k=0}^{N-1} X_k e^{j2\pi k \triangle f t}, \quad 0 \le t \le T \tag{4.1}$$

where $\triangle f$ and T denote frequency seperation and OFDM symbol duration, respectively.

Assume that OFDM signal is transmitted over AWGN channel. Let S_k be ICI coefficients defined as [36]

$$S_k = \frac{\sin \pi(k+\varepsilon)}{N \sin \frac{\pi}{N}(k+\varepsilon)} \exp\left[j\pi \left(1 - \frac{1}{N}\right)(k+\varepsilon) \right] \tag{4.2}$$

where ε denotes the normalized frequency offset. Then, the received signal at the kth subcarrier after FFT can be represented as [36]

$$y_k = X_k S_0 + \sum_{l=0, l\neq k}^{N-1} S_{l-k} X_l + n_k, \quad 0 \leq k \leq N-1 \tag{4.3}$$

where n_k denotes kth element of complex Gaussian noise.

In [36], peak interference-to-carrier ratio (PICR) is introduced to measure the resulting intercarrier interference (ICI). Then, PICR is defined as

$$\mathrm{PICR}(\mathbf{X}, \varepsilon) = \max_{0 \leq k \leq N-1} \left\{ \frac{|I_k|^2}{|S_0 X_k|^2} \right\} \tag{4.4}$$

where I_k denotes ICI on kth subcarrier and defined by

$$I_k = \sum_{l=0, l\neq k}^{N-1} S_{l-k} X_l, \quad 0 \leq k \leq N-1. \tag{4.5}$$

Note that PICR is a function of both $\mathbf{X}$ and ε.

There are some different aspects between ICI and PAPR metrics. First, ICI occurs in the receiver side. Second, unlike PAPR, ICI does not require oversampling. Third, PICR can be computed based only on a worst case value.

In [37], the upper bound of BER is derived using the maximum ICI for binary phase shift keying (BPSK). Based on this result, the relation between BER and PICR is expressed as

$$\mathrm{BER} \leq \frac{1}{4} \left[\mathrm{erfc}\left(\lambda \left(1 - \sqrt{\mathrm{PICR}} \right) \right) + \mathrm{erfc}\left(\lambda \left(1 + \sqrt{\mathrm{PICR}} \right) \right) \right] \tag{4.6}$$

where σ denotes the standard deviation of $\mathbf{X}$, $\lambda = |S_0|/\sqrt{2}\sigma$, and $\mathrm{erfc}(x) = 1 - (2/\sqrt{\pi}) \int_0^x e^{-t^2} dt$.

PICR metric can be applied to both SLM and PTS schemes instead of the PAPR metric, which leads to better BER performance.

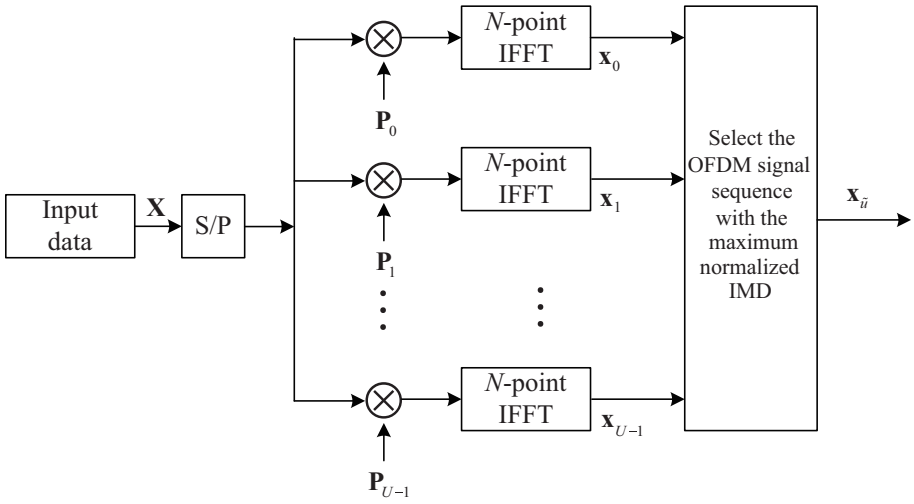

Figure 4.1: A block diagram of SLM scheme to reduce IMD [38].

4.2. IMD Reduction Scheme

In [38], intermodulation distortion (IMD) metric was proposed to enhance the error-probability performance of OFDM systems in the presence of nonlinear HPA. Fig. 4.1 shows a block diagram of SLM scheme with IMD metric. It is almost the same as the conventional SLM scheme except for the PAPR metric. Instead of PAPR metric, IMD metric is used to select the best phase sequence. Two IMD reduction criteria are considered, one with the knowledge of nonlinearity parameters and the other without it.

IMD criterion is based on the minimization over the set of possible transmit symbol vectors $\mathbf{S}$ associated with a particular information symbol vector $\mathbf{I}$ as

$$\max\left\{\max\left\{-\frac{\mathrm{Re}\{D_{k,n}^{\mathbf{S}}\}}{\mathrm{Re}\{U_{k,n}^{\mathbf{S}}\}},-\frac{\mathrm{Im}\{D_{k,n}^{\mathbf{S}}\}}{\mathrm{Im}\{U_{k,n}^{\mathbf{S}}\}}\right\},\quad n=0,\cdots,N-1\right\} \tag{4.7}$$

where $-\mathrm{Re}\{D_{k,n}^{\mathbf{S}}\}/\mathrm{Re}\{U_{k,n}^{\mathbf{S}}\}$ and $-\mathrm{Im}\{D_{k,n}^{\mathbf{S}}\}/\mathrm{Im}\{U_{k,n}^{\mathbf{S}}\}$ are in-phase and quadrature component of normalized IMD of OFDM symbol k and tone n, respectively.

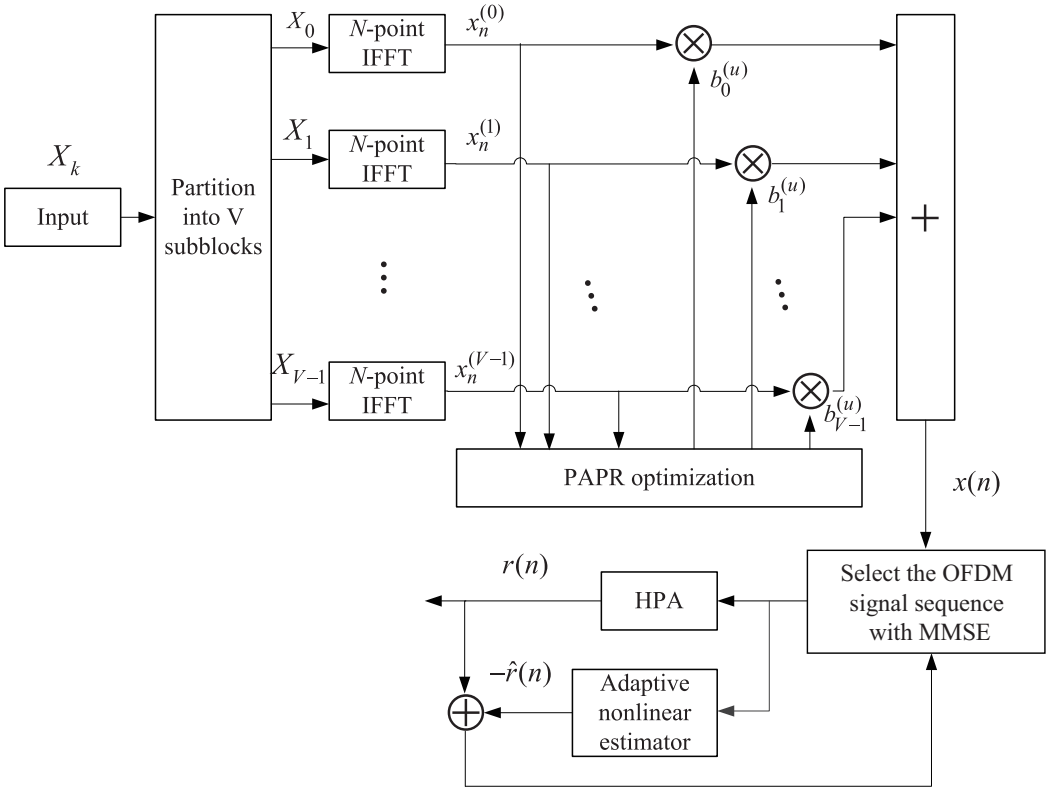

Figure 4.2: A block diagram of MSE PTS with adaptive nonlinear estimator [39].

4.3. PTS Scheme with MSE Metric

A PTS scheme using mean squared error (MSE) is proposed in [39]. Fig. 4.2 shows a block diagram of MSE PTS scheme with adaptive nonlinear estimator.

Assume that L times oversampling is used. Then, MSE is defined as

$$\text{MSE} = \sum_{n=0}^{LN-1} |x(n) - r(n)|^2 \tag{4.8}$$

where $r(n)$ is the sampled version of $r(t)$. Likewise the conventional PTS scheme, the best rotation factor is selected by MSE metric. $x(n), r(n)$, and $\hat{r}(n)$ are the OFDM

temporal signals before HPA, after HPA, and output of adaptive nonlinear estimator, respectively.

Let $d(n)$ and $\Phi_\Delta[\rho(n)]$ denote the real value amount of AM/AM and AM/PM conversions at the output of HPA at time n, respectively. In addition, $\hat{d(n)}$ and $\Phi_\Delta[\hat{\rho}(n)]$ represent amplitude and phase offset estimated by adaptive nonlinear estimator, respectively. Then, $x(n), r(n)$, and $\hat{r}(n)$ can be expressed as

$$\begin{aligned} x(n) &= \rho(n)e^{j\theta(n)} \\ r(n) &= \mathrm{A}[\rho(n)]e^{j\{\theta(n)+\Phi_\Delta[\rho(n)]\}} \\ &= d(n)\rho(n)e^{j\{\theta(n)+\Phi_\Delta[\rho(n)]\}} \\ \hat{r}(n) &= \hat{d}(n)\rho(n)e^{j\{\theta(n)+\hat{\Phi}_\Delta[\rho(n)]\}} \end{aligned} \tag{4.9}$$

where $\rho(n)$ and $\theta(n)$ denote the input signal amplitude and phase, respectively.

The updating procedures of adaptive nonlinear estimator are performed by least mean square algorithm, which are expressed as

$$\begin{aligned} d(n+1) &= \hat{d}(n) + \lambda_A[|r(n)x(n)| - \hat{d}(n)x^2(n)] \\ \hat{\Phi}_\Delta[\rho(n+1)]\} &= \hat{\Phi}_\Delta[\rho(n)] + \lambda_\Phi\{\Phi_\Delta[\rho(n)] - \hat{\Phi}_\Delta[\rho(n)]\} \end{aligned} \tag{4.10}$$

where λ_A and λ_Φ are the step sizes of adaptive algorithm.

4.4. DSR Reduction Scheme with Distortion Prediction

In [40], a PTS scheme with distortion-to-signal ratio (DSR) metric is proposed. Fig. 4.3 shows a block diagram of PTS-DSR. Assume that a third-order polynomial SSPA model is used in this study.

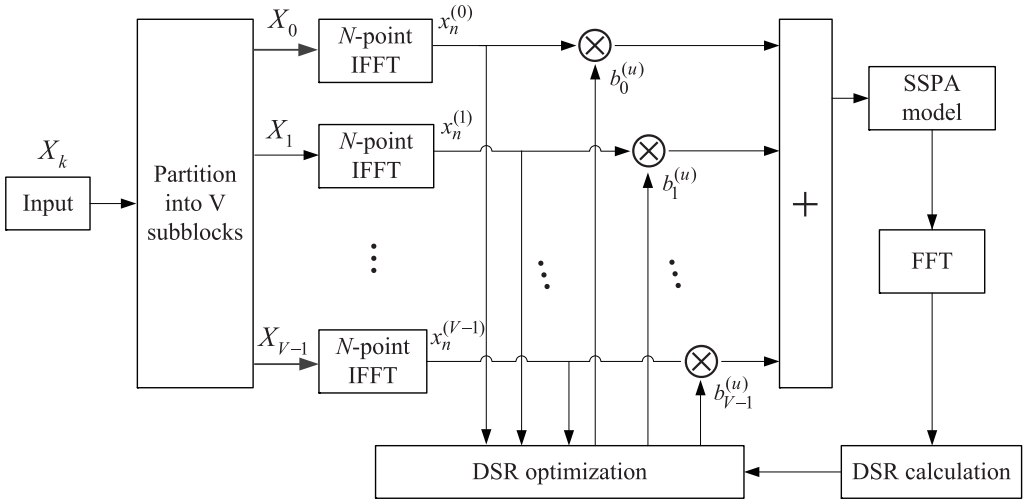

Figure 4.3: A block diagram of the PTS scheme with DSR metric [40].

Let the received signal at the kth subcarrier be y_k in the presence of nonlinear HPA as

$$y_k = \frac{1}{\sqrt{N}} \sum_{n=0}^{N-1} \left(\alpha_1 + \alpha_3 |x_n|^2\right) x_n e^{-j\frac{2\pi kn}{N}} \tag{4.11}$$

where α_1 and α_3 are the coefficients of the polynomial model. Then, y_k can be rewritten as [41]

$$y_k = \beta x_k + \psi_k \tag{4.12}$$

where ψ_k denotes the nonlinear interference component and β is real valued factor given by

$$\beta = \alpha_1 + \frac{\alpha_3}{N} \sum_{n=0}^{N-1} |x_n|^2. \tag{4.13}$$

DSR is defined in [42] as

$$\mathrm{DSR} = \frac{\mathrm{E}[|\psi|^2]}{|\beta|^2 \mathrm{E}[|\mathbf{x}|^2]}. \tag{4.14}$$

Note that the denominator is constant for a given OFDM symbol and N for normalization can be ignored. Therefore, the normalized DSR can be obtained as

$$\overline{\mathrm{DSR}} \triangleq \mathrm{E}[|\psi|^2] = \sum_{i=0}^{N-1} |\psi_i|^2. \tag{4.15}$$

The main idea of DSR-PTS is predicting the DSR by using SSPA model. Note that this method does not pass through the real HPA during the DSR calculation process. It uses simple SSPA model to reduce the computational complexity. After DSR calculation process is done, the estimated signal is passing through the real HPA and channel.

Chapter 5. Low-Complexity Class-III SLM Scheme

5.1. Introduction

OFDM is a popular multicarrier modulation technique. Because of the orthogonality of its subcarriers, a receiver can recover the transmitted data without interference. Due to its robustness against multipath fading, OFDM has been adopted as a standard technique for various wireless communication systems such as IEEE 802.11 (WLAN), IEEE 802.16 (WiMAX), and long term evolution (LTE). However, it has a high PAPR problem. When OFDM signals with high PAPR pass through nonlinear HPA, they experience in-band distortion and out-of-band radiation. Thus, in order to reduce PAPR, many schemes have been proposed such as coding [43]–[48], selected mapping (SLM) [12], partial transmit sequence [49], [50], and tone reservation [27], [51].

Because of large computational complexity by multiple IFFT operations, the conventional SLM scheme in [12] has been modified to many low-complexity SLM schemes. In [31], a low-complexity SLM scheme using set of conversion matrices was proposed. The main idea of [31] is performing one IFFT operation instead of U IFFT operations in the conventional SLM scheme. Authors in [31] found conversion matrices which have few nonzero values, which leads to low computational complexity. Then, authors in [52]

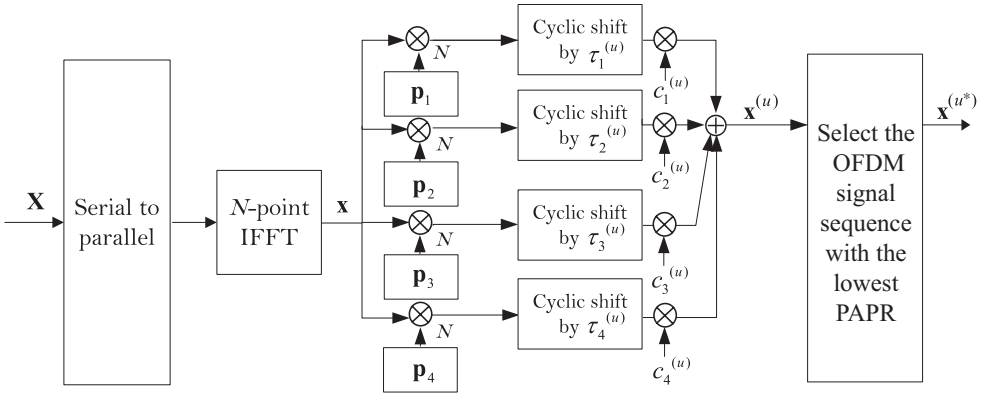

Figure 5.1: A block diagram of Class-III SLM scheme [55].

found another kind of conversion vectors which have lower computational complexity than those in [31]. Finally, three low-complexity SLM schemes using conversion vectors were proposed [55]. Among them, it is known that the one using Class-III conversion vector (which we will refer to as Class-III SLM scheme) shows better PAPR reduction performance than Class-I and Class-II SLM schemes [55]. Thus, in this chapter, we focus on Class-III SLM scheme and propose a selection method of optimal cyclic shift values by analyzing the correlation of alternative OFDM signal sequences. Note that the proposed analysis can be applied to Class-I and Class-II schemes in [55].

The rest of this chapter is organized as follows. In Section 5.2, Class-III SLM scheme is briefly overviewed. By correlation analysis, the optimal condition and the optimal cyclic shift values are proposed in Section 5.3. In Section 5.4, the required bits of side information of the proposed and random selection methods are compared. Simulation results are given in Section 5.5. Discussions and conclusions are given in Sections 5.6 and 5.7.

5.2. Overview of Class-III SLM Scheme

Fig. 5.1 shows a block diagram of Class-III SLM scheme. Clearly, it requires only one IFFT to generate all alternative OFDM signal sequences. The input symbol sequence $\mathbf{X} = [X_0, X_1, X_2, \cdots, X_{N-1}]$ to the IFFT module is usually modulated by MPSK or M-QAM, where N is the IFFT size and $N \geq 4$. The OFDM signal sequence $\mathbf{x} = [x_0, x_1, x_2, \cdots, x_{N-1}]$ is obtained by N-point IFFT of $\mathbf{X}$ and then, transformed by N-point circular convolution (denoted by $\otimes_N$) with each of four base vectors $\mathbf{p}_1$, $\mathbf{p}_2$, $\mathbf{p}_3$, and $\mathbf{p}_4$ defined as [55]

$$\begin{aligned}
\mathbf{p}_1 &= \Big[\underbrace{1,0,\cdots,0}_{\frac{N}{4}},\underbrace{1,0,\cdots,0}_{\frac{N}{4}},\underbrace{1,0,\cdots,0}_{\frac{N}{4}},\underbrace{1,0,\cdots,0}_{\frac{N}{4}}\Big] \\
\mathbf{p}_2 &= \Big[\underbrace{1,0,\cdots,0}_{\frac{N}{4}},\underbrace{j,0,\cdots,0}_{\frac{N}{4}},\underbrace{-1,0,\cdots,0}_{\frac{N}{4}},\underbrace{-j,0,\cdots,0}_{\frac{N}{4}}\Big] \\
\mathbf{p}_3 &= \Big[\underbrace{1,0,\cdots,0}_{\frac{N}{4}},\underbrace{-1,0,\cdots,0}_{\frac{N}{4}},\underbrace{1,0,\cdots,0}_{\frac{N}{4}},\underbrace{-1,0,\cdots,0}_{\frac{N}{4}}\Big] \\
\mathbf{p}_4 &= \Big[\underbrace{1,0,\cdots,0}_{\frac{N}{4}},\underbrace{-j,0,\cdots,0}_{\frac{N}{4}},\underbrace{-1,0,\cdots,0}_{\frac{N}{4}},\underbrace{j,0,\cdots,0}_{\frac{N}{4}}\Big].
\end{aligned} \tag{5.1}$$

Also, FFT of four base vectors is expressed as, i.e., $\mathbf{P}_i = \mathrm{FFT}\{\mathbf{p}_i\}$

$$\begin{aligned}
\mathbf{P}_1 &= 4\Big[\underbrace{1,0,0,0}_{4},\underbrace{1,0,0,0}_{4},\cdots,\underbrace{1,0,0,0}_{4}\Big] \\
\mathbf{P}_2 &= 4\Big[\underbrace{0,1,0,0}_{4},\underbrace{0,1,0,0}_{4},\cdots,\underbrace{0,1,0,0}_{4}\Big] \\
\mathbf{P}_3 &= 4\Big[\underbrace{0,0,1,0}_{4},\underbrace{0,0,1,0}_{4},\cdots,\underbrace{0,0,1,0}_{4}\Big] \\
\mathbf{P}_4 &= 4\Big[\underbrace{0,0,0,1}_{4},\underbrace{0,0,0,1}_{4},\cdots,\underbrace{0,0,0,1}_{4}\Big].
\end{aligned} \tag{5.2}$$

That is, FFT of four vectors are vectors interleaved partitioning the subcarriers into subgroups in PTS scheme. Therefore, Class-III-SLM scheme is exactly the same as cyclic shift PTS scheme with interleaved partitioning [54].

The ith sequence of four generated sequences is cyclically right shifted by $\tau_i^{(u)}$, $0 \le \tau_i^{(u)} < N/4$ and rotated by multiplying $c_i^{(u)} \in \{\pm 1,\ \pm j\}$, where $1 \le i \le 4$ and u is the index of alternative OFDM signal sequence. Note that without loss of generality, we can set $\tau_1^{(u)} = 0$ and $c_1^{(u)} = 1$. By summing the resulting four sequences, the uth alternative OFDM signal sequences $\mathbf{x}^{(u)}$ are generated and the one with the lowest PAPR is transmitted.

Let $\mathbf{p}^{(u)}$ be the uth Class-III conversion vector to generate $\mathbf{x}^{(u)}$, which is given as

$$\mathbf{p}^{(u)} = \sum_{i=1}^{4} c_i^{(u)} \mathbf{p}_{i\langle \tau_i^{(u)} \rangle} \tag{5.3}$$

where $\mathbf{p}_{i\langle \tau_i^{(u)} \rangle}$ denotes the cyclic-shifted version of $\mathbf{p}_i$ to the right by $\tau_i^{(u)}$. It is clear that $\mathbf{x}^{(u)}$ is generated by $\mathbf{x}^{(u)} = \mathbf{p}^{(u)} \otimes_N \mathbf{x}$.

Class-III SLM scheme can generate up to $(N/4)^3 4^3 = N^3$ alternative OFDM signal sequences by varying $\tau_i^{(u)}$ and $c_i^{(u)}$. Since N^3 is a large number in practice, a deterministic selection method of a good subset of $\tau_i^{(u)}$'s and $c_i^{(u)}$'s is needed, which results in

good PAPR reduction performance. In the next section, such selection method will be proposed.

5.3. Selection of Optimal Alternative OFDM Signal Sequences for Class-III SLM Scheme

In the previous section, we showed that Class-III-SLM scheme is exactly the same as CS-PTS scheme with interleaved partitioning. It is known that the PTS scheme with random partitioning shows good PAPR reduction performance. However, the PTS scheme with interleaved partitioning shows bad PAPR reduction performance because the subcarriers are highly correlated. Therefore, the correlation analysis in the following section is essential for Class-III-SLM scheme.

5.3.1. Correlation Analysis

The magnitude of the correlation $R_{st}(m)$ between the sth and the tth alternative OFDM signal sequences is defined as

$$\begin{aligned}\left|R_{st}(m)\right| &= \left|E\{x_n^{(s)} x_{n+m}^{(t)*}\}\right| \\ &= \frac{1}{N^2}\left|E\left\{\sum_{k=0}^{N-1}|X_k|^2 P_k^{(s)} P_k^{(t)*} e^{-j\frac{2\pi}{N}km}\right\}\right| \\ &= \frac{1}{N^2}\left|\sum_{k=0}^{N-1} P_k^{(s)} P_k^{(t)*} e^{-j\frac{2\pi}{N}km}\right| \end{aligned} \tag{5.4}$$

where $x_n^{(s)}$ denotes the nth element of the sth alternative OFDM signal sequence, $P_k^{(s)}$ denotes the kth element of the sth phase sequence $\mathbf{P}^{(s)} = \mathrm{FFT}\{\mathbf{p}^{(s)}\}$, $(\cdot)^*$ denotes the complex conjugation, and $-(N-1) \le m \le N-1$. X_k's are assumed to be independent

and identically distributed with $E\{|X_k|^2\} = 1$. Therefore, $E\{X_k X_e^*\} = 1$ if $k = e$, otherwise $E\{X_k X_e^*\} = 0$. Since $|R_{st}(m)|$ is symmetric about m, analyzing $|R_{st}(m)|$ over $0 \leq m \leq N-1$ is enough [53].

The uth alternative OFDM signal sequence of Class-III SLM scheme is expressed as

$$\begin{aligned}\mathbf{x}^{(u)} &= \mathbf{p}^{(u)} \otimes_N \mathbf{x} \\ &= \left(\sum_{i=1}^{4} c_i^{(u)} \mathbf{p}_{i\langle \tau_i^{(u)} \rangle} \right) \otimes_N \mathbf{x} \\ &= \mathrm{IFFT} \left\{ \left(\sum_{i=1}^{4} c_i^{(u)} \mathbf{P}_i{}^{\left(\tau_i^{(u)}\right)} \right) \odot \mathbf{X} \right\} \end{aligned} \tag{5.5}$$

where $\mathbf{P}_i{}^{(\tau_i^{(u)})} \equiv \mathrm{FFT}\{\mathbf{p}_{i\langle \tau_i^{(u)} \rangle}\}$ and $\odot$ denotes the componentwise multiplication of vectors. It is clear that $\sum_{i=1}^{4} c_i^{(u)} \mathbf{P}_i{}^{\left(\tau_i^{(u)}\right)}$ can be regarded as a phase sequence. Therefore, Class-III SLM scheme is the conventional SLM scheme using the following $\mathbf{P}^{(u)}$ as the uth phase sequence

$$\mathbf{P}^{(u)} = \sum_{i=1}^{4} c_i^{(u)} \mathbf{P}_i{}^{\left(\tau_i^{(u)}\right)}. \tag{5.6}$$

More specifically, $\mathbf{P}_i = \mathrm{FFT}\{\mathbf{p}_i\}$ and $c_i^{(u)} \mathbf{P}_i{}^{\left(\tau_i^{(u)}\right)}$ are

$$\mathbf{P}_i = 4\Big[\underbrace{0, \cdots, 0}_{i-1}, \underbrace{1, 0, 0, 0}_{4}, \underbrace{1, 0, 0, 0}_{4}, \cdots, \underbrace{0, \cdots, 0}_{4-i}\Big],$$

$$c_i^{(u)} \mathbf{P}_i{}^{\left(\tau_i^{(u)}\right)} = 4\Big[\underbrace{0, \cdots, 0}_{i-1}, \cdots, \underbrace{c_i^{(u)} e^{-j\frac{2\pi}{N}\tau_i^{(u)}}, 0, 0, 0}_{4}, \cdots, \underbrace{0, \cdots, 0}_{4-i}\Big].$$

Now, we obtain the uth phase sequence in (5.6) as

$$\mathbf{P}^{(u)} = 4\Big[P_0^{(u)}, P_1^{(u)}, \cdots, P_{N-1}^{(u)}\Big] \tag{5.7}$$

where

$$P_k^{(u)} = \begin{cases} c_1^{(u)} e^{-j\frac{2\pi}{N}k\tau_1^{(u)}}, & k = 0 \bmod 4 \\ c_2^{(u)} e^{-j\frac{2\pi}{N}k\tau_2^{(u)}}, & k = 1 \bmod 4 \\ c_3^{(u)} e^{-j\frac{2\pi}{N}k\tau_3^{(u)}}, & k = 2 \bmod 4 \\ c_4^{(u)} e^{-j\frac{2\pi}{N}k\tau_4^{(u)}}, & k = 3 \bmod 4\,. \end{cases} \tag{5.8}$$

By plugging (5.8) into (5.4), the inner part $\mathrm{A}(m)$ of the magnitude $|\cdot|$ in (5.4) is expressed as

$$\begin{aligned} \mathrm{A}(m) &= \sum_{k=0}^{N-1} P_k^{(s)} P_k^{(t)*} e^{-j\frac{2\pi}{N}km} \\ &= 16 \sum_{v=0}^{\frac{N}{4}-1} \sum_{i=1}^{4} c_i^{(s)} c_i^{(t)*} e^{-j\frac{2\pi}{N}(4v+i-1)\left(m-(\tau_i^{(t)}-\tau_i^{(s)})\right)} \\ &= 16 \sum_{i=1}^{4} \mathrm{A}_i(m) \end{aligned} \tag{5.9}$$

where $\mathrm{A}_i(m)$ is defined as

$$\begin{aligned} \mathrm{A}_i(m) &= c_i^{(s)} c_i^{(t)*} \sum_{v=0}^{\frac{N}{4}-1} e^{-j\frac{2\pi}{N}(4v+i-1)\left(m-(\tau_i^{(t)}-\tau_i^{(s)})\right)} \\ &= c_i^{(s)} c_i^{(t)*} \bar{\mathrm{A}}_i(m). \end{aligned} \tag{5.10}$$

If $m - (\tau_i^{(t)} - \tau_i^{(s)})$ is a multiple of $N/4$, then $|\bar{\mathrm{A}}_i(m)| = N/4$. Otherwise, it is zero. Let $d_{st}(\tau_i) = \tau_i^{(t)} - \tau_i^{(s)} \bmod N/4$. Then, the values of $\bar{\mathrm{A}}_i(m)$ for all m are listed in Table 5.1.

In Fig. 5.2, $|\bar{\mathrm{A}}_i(m)|$ is expressed. Each $|\bar{\mathrm{A}}_i(m)|$ has four nonzero values, i.e.,$|\bar{\mathrm{A}}_i(m)| = N/4$. Also, the position of nonzero values is defined by $d_{st}(\tau_i)$.

Table 5.1: $\bar{\mathrm{A}}_i(m)$ for all m.

m	$d_{st}(\tau_i)$	$\frac{N}{4}+d_{st}(\tau_i)$	$\frac{2N}{4}+d_{st}(\tau_i)$	$\frac{3N}{4}+d_{st}(\tau_i)$	Otherwise
$\bar{\mathrm{A}}_1(m)$	$\frac{N}{4}$	$\frac{N}{4}$	$\frac{N}{4}$	$\frac{N}{4}$	0
$\bar{\mathrm{A}}_2(m)$	$\frac{N}{4}$	$-\frac{N}{4}j$	$\frac{N}{4}$	$\frac{N}{4}j$	0
$\bar{\mathrm{A}}_3(m)$	$\frac{N}{4}$	$-\frac{N}{4}$	$\frac{N}{4}$	$-\frac{N}{4}$	0
$\bar{\mathrm{A}}_4(m)$	$\frac{N}{4}$	$\frac{N}{4}j$	$\frac{N}{4}$	$-\frac{N}{4}j$	0

5.3.2. Selection of Optimal Cyclic Shift Values

In [53], it is shown that a set of U phase sequences with low variance of correlation (VC) in SLM scheme gives good PAPR reduction performance. Since there is no analytical result when the phase sequences are correlated. Therefore, we use the heuristic criterion in [53]. VC is defined as

$$\mathrm{VC}=\left(\sum_{0\le s<t\le U-1}\mathrm{Var}\left\{\left|R_{st}(m)\right|^2\right\}_{m=0}^{N-1}\right)/\binom{U}{2} \tag{5.11}$$

where Var$\{\cdot\}$ denotes the variance. VC is the average of variance of magnitude of correlation values. Low VC means that alternative OFDM signal sequences are low correlated. Since the conventional SLM scheme shows good PAPR reduction performance when alternative OFDM signal sequences are low correlated, VC can be a good criterion for Class-III SLM scheme. Based on VC, we derive the optimal condition for cyclic shift values of Class-III SLM.

Theorem 1. *If the cyclic shift values satisfy* $d_{st}(\tau_i)\neq d_{st}(\tau_{i'})$ *mod* $N/4$ *for all* $\binom{U}{2}$ *pairs of alternative OFDM signal sequences, where* $1\le s<t\le U$ *and* $1\le i\neq i'\le 4$,

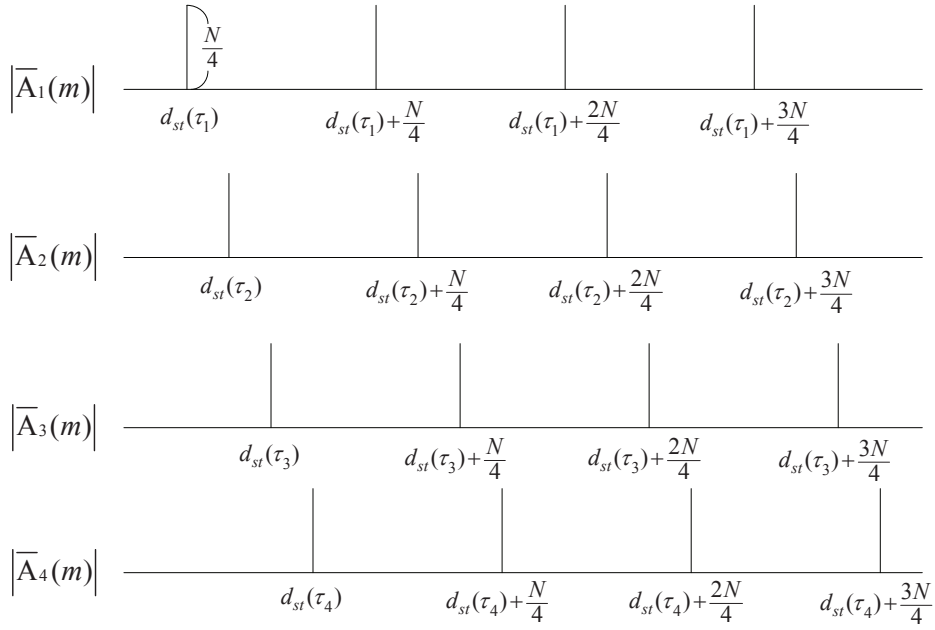

Figure 5.2: Expression of $|\bar{\mathrm{A}}_i(m)|$.

then the OFDM signal sequences are optimal in terms of minimizing VC.

Proof. Note that each $\bar{\mathrm{A}}_i(m)$ has four nonzero values for all $0 \leq m \leq N-1$ (see Table 5.1). Suppose that $d_{st}(\tau_1) = d_{st}(\tau_2) = d_{st}(\tau_3) \neq d_{st}(\tau_4)$. Then, when $m = d_{st}(\tau_1)$, $\bar{\mathrm{A}}_1(m) = \bar{\mathrm{A}}_2(m) = \bar{\mathrm{A}}_3(m) = N/4$, i.e., $\mathrm{A}(m) = 3N/4$ if $c_i^{(s)} c_i^{(t)*} = 1$. On the other hand, if $d_{st}(\tau_1) \neq d_{st}(\tau_2) \neq d_{st}(\tau_3) \neq d_{st}(\tau_4)$, then $\mathrm{A}(m) = N/4$. That is, the same differences of cyclic shift values increase VC even if $c_i^{(s)} c_i^{(t)*} \neq 1$. Therefore, to minimize VC, it is required that $d_{st}(\tau_i) \neq d_{st}(\tau_{i'}) \bmod N/4$ for all $\binom{U}{2}$ pairs of alternative OFDM signal sequences. □

Note that VC only depends on $d_{st}(\tau_i)$, not on $c_i^{(s)} c_i^{(t)*}$ because the rotation by multi-

plying $c_i^{(u)}$ does not change the energy. Therefore, the rotation value does not affect the PAPR reduction performance in this case.

Based on the optimal condition, a simple selection of the optimal cyclic shift values satisfying the optimal condition is proposed in Table 5.2, where u is the index of alternative OFDM signal sequence.

The probability that randomly selected cyclic shift values do not satisfy the optimal condition is

$$1 - \left\{ \frac{4!\binom{N/4}{4}}{(N/4)^4} \right\}^{\binom{U}{2}} \tag{5.12}$$

where $\binom{n}{k}$ denotes k-combinations of a set n, i.e.,$\binom{n}{k} = n!/k!(n-k)!$. When $N = 256$ and $U = 4$, the probability is 0.4362. However, many of those 43.62% cases show fairly good performance because they satisfy the near optimal condition for many pairs even if not for all pairs. For example, there are 6 pairs of alternative OFDM signal sequences to be checked for satisfying the optimal condition in Theorem 1. Suppose that 5 pairs satisfy the optimal condition and one pair does not. Then, this case corresponds to the 43.62% cases, but it may show good performance due to the 5 optimal pairs. Therefore, it is possible that the performance of the proposed scheme gives little enhancement from simulation results.

However, 43.62% is not negligible, and thus, deterministic selection of optimal cyclic shift values is important.

5.3.3. Maximum Number of Optimal Alternative OFDM Signal Sequences

The next theorem derives the maximum number of optimal alternative OFDM signal sequences for Class-III SLM scheme.

Table 5.2: Selection of optimal cyclic shift values.

u	1	2	3	$\cdots$	k
$\tau_1^{(u)}$	0	0	0	$\cdots$	0
$\tau_2^{(u)}$	1	2	3	$\cdots$	k mod $\frac{N}{4}$
$\tau_3^{(u)}$	2	4	6	$\cdots$	$2k$ mod $\frac{N}{4}$
$\tau_4^{(u)}$	3	6	9	$\cdots$	$3k$ mod $\frac{N}{4}$

Theorem 2. *When the optimal cyclic shift values in Table 5.2 are used for $N = 2^m$ with $m > 2$, the maximum number of optimal alternative OFDM signal sequences is $N/8$.*

Proof. Let s and t be the indices of alternative OFDM signal sequences and $0 < s < t < U$. Then, the corresponding differences of cyclic shift values are $d_{st}(\tau_1) = 0$, $d_{st}(\tau_2) = t - s$, $d_{st}(\tau_3) = 2(t - s)$, and $d_{st}(\tau_4) = 3(t - s) = 2(t - s) + (t - s)$, respectively. Now, we consider two cases.

Case 1) $\max(t - s) < N/8$;

Note that $d_{st}(\tau_{i'}) - d_{st}(\tau_i) = k(t-s)$ mod $N/4$, where $i, i' \in \{1, 2, 3, 4\}, i < i'$, and $k = i' - i \in \{1, 2, 3\}$. When $k = 1$ or 2, $d_{st}(\tau_{i'}) - d_{st}(\tau_i) \neq 0$ because $2(t-s) < N/4$. When $k = 3$, $d_{st}(\tau_4) - d_{st}(\tau_1) = 3(t - s) < 3N/8$. We have to check whether $3(t - s)$ can be either 0 or $N/4$ which are the cases of $d_{st}(\tau_4) = d_{st}(\tau_1)$. It is clear that $3(t - s) \neq 0$ by $s < t$ and $3(t - s) \neq 2^{m-2} = N/4$. Thus, the optimal condition $d_{st}(\tau_i) \neq d_{st}(\tau_{i'})$ mod $N/4$ always hold for Case 1).

Table 5.3: Another cyclic shift values satisfying the optimal condition.

u	1	2	3	$\cdots$	k
$\tau_1^{(u)}$	0	0	0	$\cdots$	0
$\tau_2^{(u)}$	1	2	3	$\cdots$	k mod $\frac{N}{4}$
$\tau_3^{(u)}$	2	4	6	$\cdots$	$3k$ mod $\frac{N}{4}$
$\tau_4^{(u)}$	3	6	9	$\cdots$	$5k$ mod $\frac{N}{4}$

Case 2) $\max(t-s) \geq N/8$;

Suppose that $t - s = N/8$. Then, $d_{st}(\tau_2) = d_{st}(\tau_4)$ mod $N/4$. Thus, Case 2) does not satisfy the optimal condition. □

Note that Table 5.2 is not the unique solution satisfying the optimal condition. For example, Table 5.3 also satisfies the optimal condition in Theorem 1. However, the maximum number of optimal alternative OFDM signal sequences is $N/16$, not $N/8$. For the given number of alternative OFDM signal sequences, there are several number of optimal selection methods. We are not sure whether the proposed selection method in Table 5.2 is the best choice or not in terms of the number of optimal alternative OFDM signal sequences. However, we think that $N/8$ is big enough for Class-III SLM scheme or the conventional SLM scheme. For example, 128 optimal alternative OFDM signal sequences can be generated by Table 5.2 when $N = 1024$.

5.3.4. Selection of Additional Alternative OFDM Signal Sequences

In Theorem 2, it is shown that the maximum number of optimal alternative OFDM signal sequences is $N/8$. However, it may be necessary to generate more alternative OFDM signal sequences by sacrificing the optimality. Thus, a simple method to generate good additional alternative OFDM signal sequences is proposed by properly adjusting the rotation values. For good PAPR reduction performance, we only consider $c_1^{(u)} \neq c_2^{(u)} \neq c_3^{(u)} \neq c_4^{(u)}$.

Let us consider a case of generating $N/4$ alternative OFDM signal sequences. In Section III-B, $N/8$ optimal alternative OFDM signal sequences without rotation values can be generated. However, by adjusting the rotation values for these $N/8$ optimal alternative OFDM signal sequences, good additional $N/8$ alternative OFDM signal sequences can be generated. Note that the same cyclic shift values in Table 5.2 are used for the first $N/8$ optimal sequences and the second additional $N/8$ sequences. For example, to generate total $N/4$ alternative OFDM signal sequences, the rotation values $c_1^{(u)} = 1, c_2^{(u)} = -1, c_3^{(u)} = j$, and $c_4^{(u)} = -j$ are multiplied to each of the $N/8$ optimal alternative OFDM signal sequence cases to generate additional $N/8$ sequences.

Let $c_i^{(u)} = e^{j\theta_i^{(u)}}$, and if we use $\theta_i^{(u)} = (i-1)(\pm\pi/2)$ or $(i-1)\pi$ for the second $N/8$ alternative OFDM signal sequences, the PAPR reduction performances of the first $N/8$ and the second $N/8$ sequences are the same because the second $N/8$ sequences are just cyclic-shifted version of the first $N/8$ optimal sequences in time domain. Therefore, to generate good additional alternative OFDM signal sequences, we need to use the rotation values which do not have linear relation as above. Consequently, total $4N/8$ good alternative OFDM signal sequences can be generated by multiplying the rotation values $\{c_1^{(u)}, c_2^{(u)}, c_3^{(u)}, c_4^{(u)}\} = \{1, j, -j, -1\}, \{1, -j, j, -1\}, \{1, -1, j, -j\}, \{1, -1, -j, j\}$ to

Table 5.4: Rotation values which do not have linear relation.

Number	$\{c_1^{(u)}, c_2^{(u)}, c_3^{(u)}, c_4^{(u)}\}$
1	$\{1, j, -j, -1\}$
2	$\{1, -j, j, -1\}$
3	$\{1, -1, j, -j\}$
4	$\{1, -1, -j, j\}$

each of the $N/8$ optimal sequences. These rotation values are listed in Table 5.4.

5.4. Side Information

Random scheme requires $\lceil \log_2 (N/4)^3 \rceil$ bits of side information for cyclic shift values and $\lceil \log_2 4^3 \rceil$ bits of side information for rotation values. Whereas, the proposed scheme requires only $\lceil \log_2 U \rceil$ bits of side information if the cyclic shift values in Table 5.2 are shared by transmitter and receiver. Table 5.5 shows the required side information bits when $N = 64,\ 256$, and 1024 and $U = 4,\ 8$, and 16. Note that the side information for the proposed scheme is a function of U. Whereas, that of random scheme is a function of N. Since $N \gg U$, that of random scheme is much larger than the proposed scheme. Assume that 16-QAM modulation is used. Then, 4 bits (one symbol) of side information is required for the proposed scheme when $N = 1024$ and $U = 16$. Whereas, that of the random scheme is 30 bits (8 symbols). Therefore, the proposed scheme requires much less side information than the random scheme.

Table 5.5: Side information comparisons of the proposed and the random schemes.

N	U	Proposed	Random (cyclic and rotation values)
64	4	2	$18\ (12+6)$
	8	3	
	16	4	
256	4	2	$24\ (18+6)$
	8	3	
	16	4	
1024	4	2	$30\ (24+6)$
	8	3	
	16	4	

5.5. Simulation Results

In this section, we compare the PAPR reduction performances of Class-III SLM scheme by random selection and the proposed selection of the cyclic shift and rotation values. For random selection, cyclic shift and rotation values are randomly selected from $0 \leq \tau_i^{(u)} < N/4$ and $c_i^{(u)} \in \{\pm 1, \pm j\}$, and for the proposed scheme, rotation values are not used to generate $N/8$ optimal alternative OFDM signal sequences.

In Fig. 5.3, Proposed selection I and Proposed selection II use the cyclic shift values in Table 5.2 and $\tau_1^{(u)} = 0$, $\tau_2^{(u)} = k$, $\tau_3^{(u)} = 3k$, and $\tau_4^{(u)} = 5k$, which also satisfies the

optimal condition, respectively. When $N = 64,\ 256$ and $U = 4$, the PAPR reduction performances of random scheme are degraded compared to the proposed scheme. When U and N are large, the performance gap becomes negligible. Proposed selections I and II show the identical PAPR reduction performance. Since random scheme satisfies the near optimal condition for many pairs of alternative OFDM signal sequences, it is possible that the proposed scheme shows little performance enhancement. However, we can find that the proposed scheme shows the optimal PAPR reduction performance.

In Fig. 5.4, ROT-I denotes the case of using $c_1^{(u)} = 1, c_2^{(u)} = -1, c_3^{(u)} = j, c_4^{(u)} = -j$ for generating additional $N/8$ alternative OFDM signal sequences. ROT-II denotes the case of using $c_1^{(u)} = 1, c_2^{(u)} = j, c_3^{(u)} = -1, c_4^{(u)} = -j$ for generating additional $N/8$ alternative OFDM signal sequences. The proposed selection ROT-I with $U = N/4$ shows almost the same PAPR reduction performance as random selection with $U = N/4$. This means that good additional alternative OFDM signal sequences can be generated by the proposed method ROT-I. Note that the same cyclic shift values in Table 5.2 are used for the first optimal $N/8$ and the second additional $N/8$ sequences with different rotation values. Whereas, the proposed selection ROT-II with $U = N/4$ shows almost the same PAPR reduction performance as the random selection with $U = N/8$ because the rotation values have linear relation, which causes no additional PAPR reduction gain for ROT-II.

Selection-I ($d_{st}(\tau_1) = d_{st}(\tau_2)$) and Selection-II ($d_{st}(\tau_1) = d_{st}(\tau_2) = d_{st}(\tau_3)$) are also considered to show the performance degradation from bad selection of the cyclic shift values.

Fig. 5.5 compares the PAPR reduction performances of Class-III SLM scheme by Random selection, Proposed selection, Selection-I, and Selection-II. The PAPR reduc-

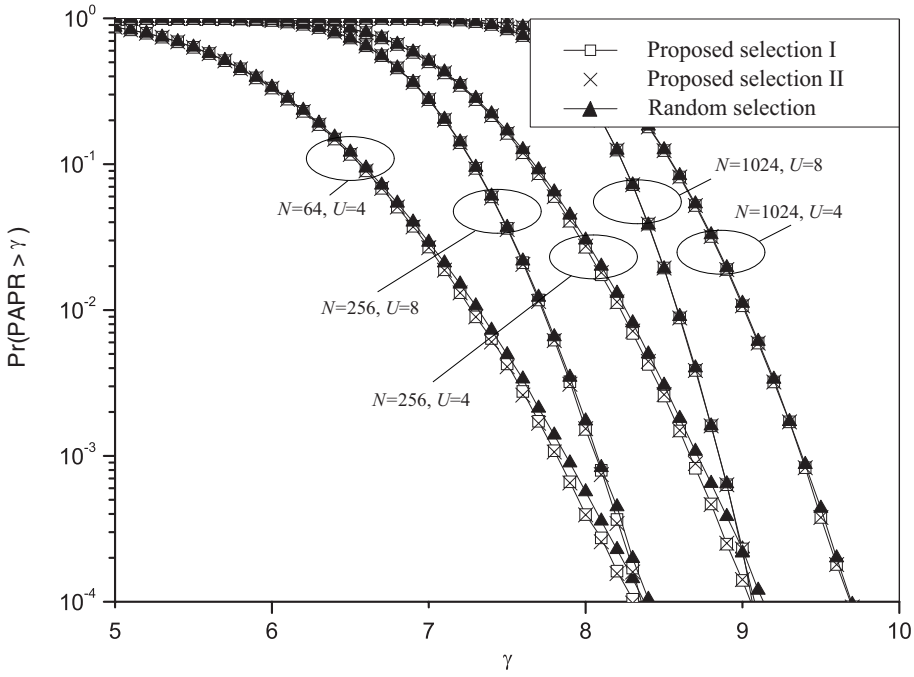

Figure 5.3: Comparison of PAPR reduction performance of Class-III SLM scheme by Random selection and Proposed selections I and II when 16-QAM, $N = 64, 256, 1024$, and $U = 4$ and 8 are used.

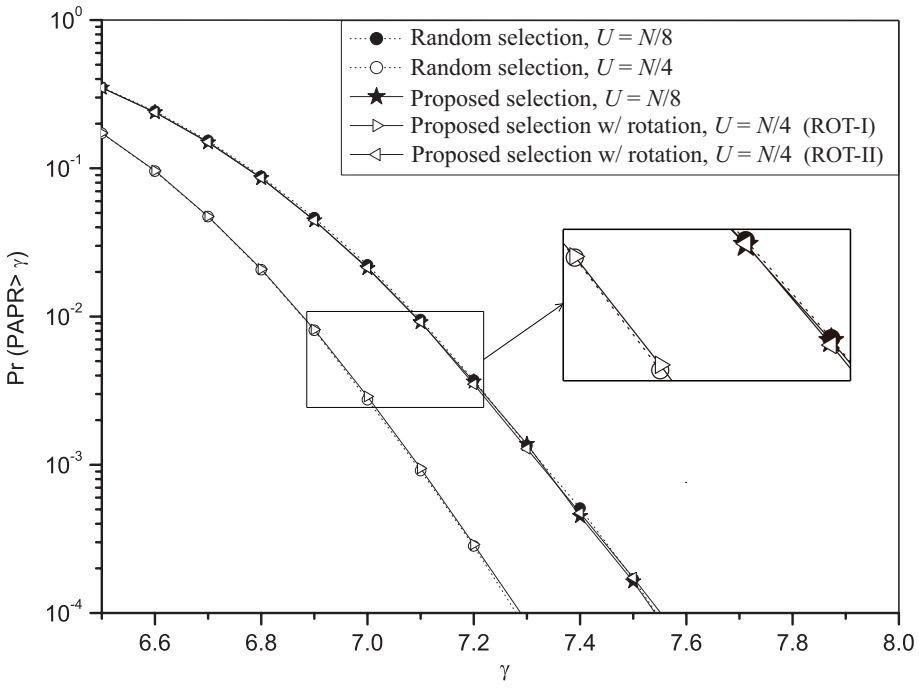

Figure 5.4: Comparison of PAPR reduction performance of Class-III SLM scheme by Random selection and Proposed selections with ROT-I and ROT-II when 16-QAM, $N = 256$, and $U = N/8$ or $N/4$ are used.

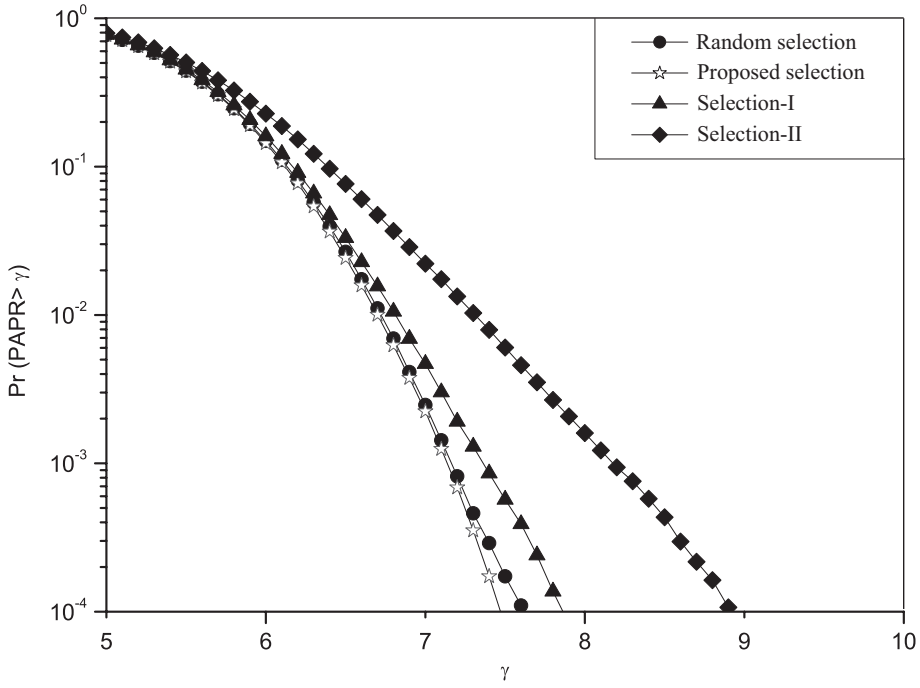
Random selection
Proposed selection
Selection-I
Selection-II
Pr (PAPR> γ)
γ
10^0
10^-1
10^-2
10^-3
10^-4
5
6
7
8
9
10

(a)

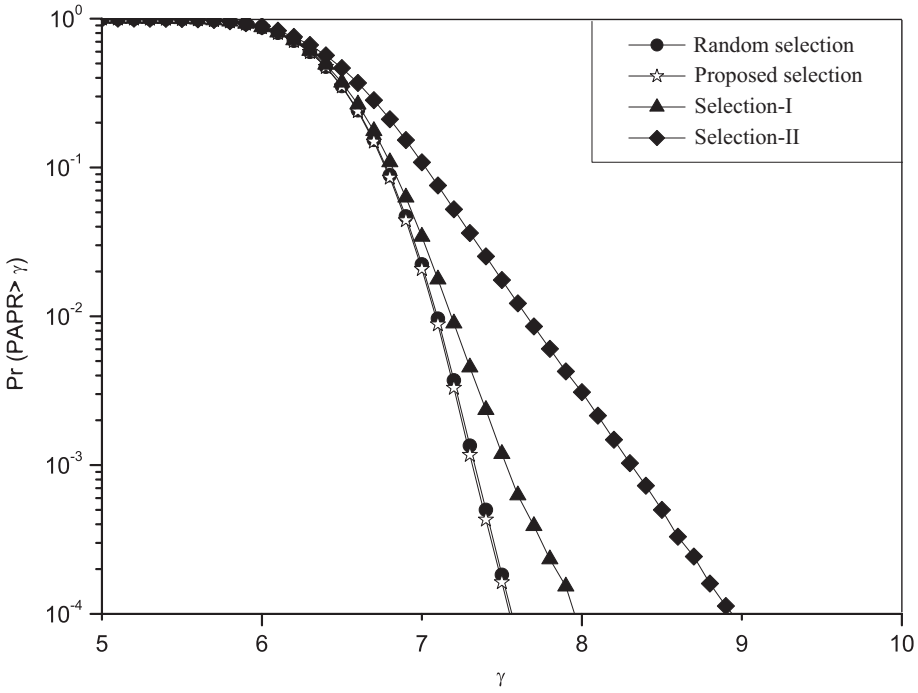
Random selection
Proposed selection
Selection-I
Selection-II
Pr (PAPR> γ)
γ
10^0
10^-1
10^-2
10^-3
10^-4
5
6
7
8
9
10

(b)

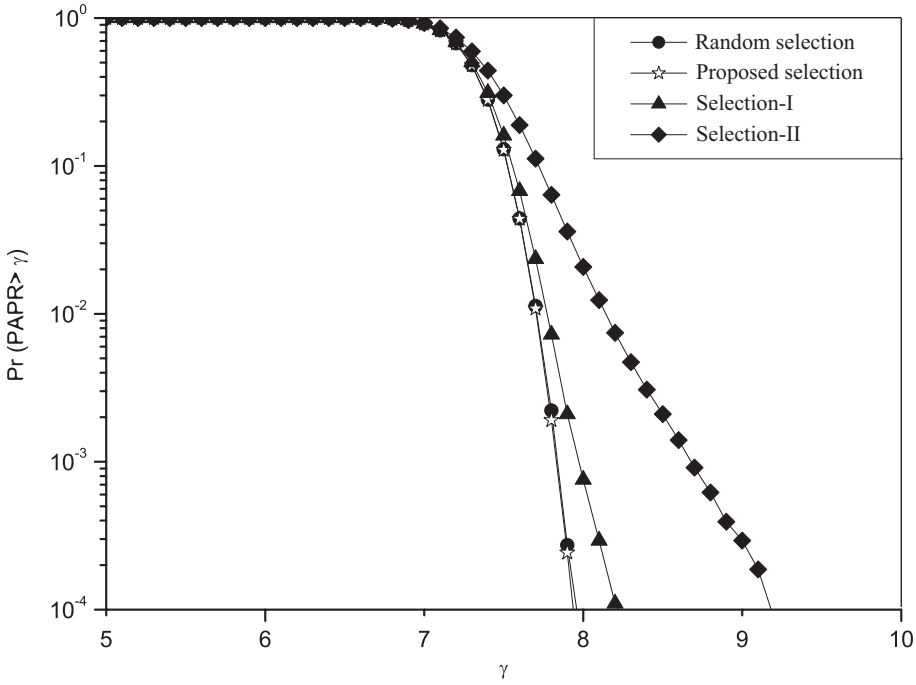

(c)

Figure 5.5: Comparison of PAPR reduction performance of Class-III SLM scheme by Random selection, Proposed selection, Selection-I, and Selection-II when: (a) $N = 64$, (b) $N = 64$, and (c) $N = 1024$.

tion performances of Selection-I and Selection-II are much worse than Proposed selection and Random selection for $N = 64,\ 256$ and 1024. Also, the PAPR reduction performance of Selection-II is worse than Selection-I because the most of cases in Selection-II do not satisfy the optimal condition.

It is also shown that Proposed selection achieves the best PAPR reduction performance. In general, the random selection scheme does not guarantee the optimal PAPR reduction performance. As you can see in Fig. 5.5, the random selection scheme can be either Selection-I or Selection-II (bad cases), which show poor PAPR reduction performance. However, the proposed selection scheme is a deterministic scheme and always guarantees the optimal PAPR reduction performance.

5.6. Discussions

The basic idea of Class-III SLM scheme is using circular convolution operation instead of IFFT operation. Therefore, this idea can be applied to other SLM schemes such as the conventional SLM scheme and CORR SLM scheme. Also, as we mentioned, Class-III SLM scheme is identical to cyclic-shift PTS scheme. Due to the correlations between subcarriers in the same subblock, it causes PAPR reduction performance degradation.

The proposed scheme is optimal in terms of lowest VC, because the same differences of cyclic shift values increase the variance. Note that there is no optimal criterion to achieve the optimal PAPR reduction performance when phase sequences are correlated. However, VC criterion is confirmed by simulation results that SLM scheme with low VC phase sequences shows good PAPR reduction performance. Therefore, VC criterion is used in this study.

In the simulation result, the practical parameters are used such as $N = 1024$ and $U = 4$ and 8. Therefore, the proposed scheme guarantees good PAPR reduction performance in the practical area.

5.7. Conclusions

In this study, a selection method of optimal cyclic shift values for Class-III SLM scheme is proposed. Also, a selection method of good additional alternative OFDM signal sequences by using proper rotation values is proposed.

Although the analysis to derive the optimal condition is complicated, we do not need to compute the optimal condition for each OFDM symbol when we apply the proposed scheme to OFDM systems. To use the proposed scheme, we only need to use U predetermined optimal cyclic shift values given in Table 5.2. Therefore, the computational complexity of the proposed scheme is basically the same as the random scheme.

There are some advantages of the proposed scheme. First, the random scheme requires memory for 3 complex numbers (rotation values), whereas the proposed scheme does not need the memory for rotation values. Second, the random scheme requires $\lceil \log_2 (N/4)^3 \rceil$ bits of side information for cyclic shift values and $\lceil \log_2 4^3 \rceil$ bits of side information for rotation values. Whereas, the proposed scheme requires only $\lceil \log_2 U \rceil$ bits of side information if the cyclic shift values in Table 5.2 are shared by transmitter and receiver. Table 5.5 shows the required side information bits when $N = 64,\ 256$, and 1024 and $U = 4,\ 8$, and 16. Note that the side information for the proposed scheme is a function of U, whereas that of the random scheme is a function of N. Since $N \gg U$, that of the random scheme is much larger than the proposed scheme. Assume that 16-

QAM modulation is used. Then, 4 bits (one symbol) of side information is required for the proposed scheme when $N = 1024$ and $U = 16$. Whereas, that of the random scheme is 30 bits (8 symbols). Therefore, the proposed scheme requires much less side information than random scheme. Third, the random scheme has a risk to select the cases of bad PAPR reduction performance, whereas the proposed scheme always guarantees the optimal PAPR reduction performance in terms of minimizing VC.

Note that Class-III-SLM scheme is exactly the same as cyclic shift PTS scheme [54]. Therefore, this analysis can be adopted to other methods in [55] and cyclic shift PTS schemes.

Chapter 6. Low-Complexity CORR SLM Scheme

6.1. Introduction

OFDM has been widely used in various wireless communication systems. Since OFDM signals show high PAPR, many schemes have been proposed to mitigate the PAPR problem. Among them, PTS and SLM schemes can be good answers to solve the PAPR problem, where many alternative OFDM signals are generated and the one with the minimum PAPR is selected for transmission. Since these schemes have high computational complexity due to multiple IFFT operations, many low-complexity schemes have been proposed.

While above schemes focus on reducing the PAPR metric, many other metrics are proposed to improve the BER performance in the presence of nonlinear devices such as HPA. It is known that intermodulation distortion [38], distortion-to-signal power ratio [40], mean squared error [39], and correlation (CORR) metrics [56] outperform the PAPR metric in terms of BER performance of OFDM systems. Except for the PAPR metric, CORR metric shows the lowest computational complexity while its BER performance is almost the same as those of other metrics. Although CORR shows relatively high PAPR than PAPR metric, BER performance of CORR metric can be enhanced com-

pared to the PAPR metric.

In this chapter, we will investigate oversampling rate required to show the similar performance as the continuous OFDM signal case. By calculating the correlation coefficients of the result sequences after computing CORR metric for the continuous and the oversampled cases, proper oversampling rate can be derived.

The rest of this chapter is organized as follows. In Section 6.2, CORR SLM scheme is briefly reviewed and it is shown that CORR metric is near optimal in terms of BER performance. In Section 6.3, the oversampling effect is analyzed for the SLM scheme using CORR metric in the presence of nonlinear HPA by computing CORR metric and Pearson correlation coefficient values. Computational complexity of CORR SLM scheme with two and four times oversampling cases is compared in Section 6.4. Then, the effect of the HPA coefficient α_3 is shown in Section 6.6. Simulation results are shown in Section 6.5. Finally, conclusions are given in Section 6.7.

6.2. Overview of SLM Scheme Using CORR Metric

6.2.1. Overview of CORR Metric

Binary data sequences are modulated by MQAM to generate an input symbol sequence $[X_0, X_1, \cdots, X_{N-1}]$. Then, $(L-1)N$ zeros are padded to the end (or middle) of the input symbol sequence, which is called L times oversampling, as

$$\mathbf{X} = [X_0, X_1, \cdots, X_{N-1}, \underbrace{0, \cdots, 0}_{(L-1)N \ 0'\text{s}}] \tag{6.1}$$

where N is the number of subcarriers and L is the oversampling factor. In general, it is

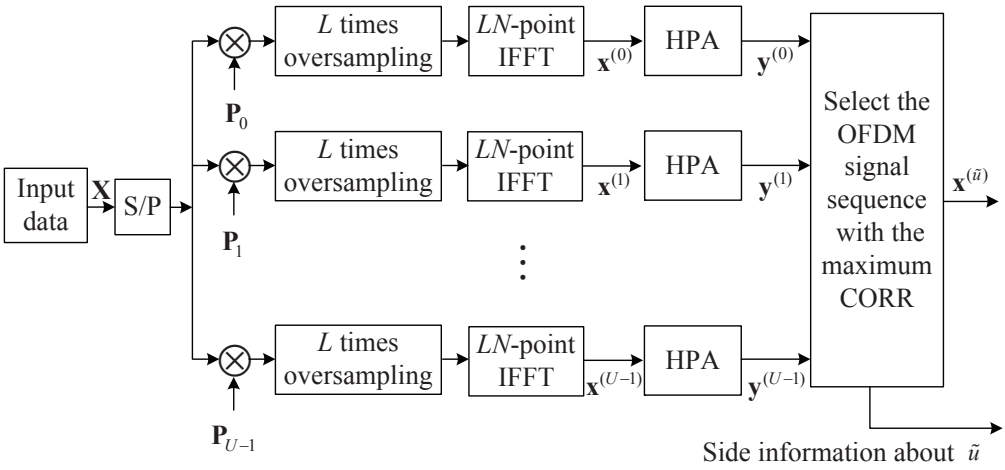

Figure 6.1: A block diagram of the SLM scheme using CORR metric [56].

known that four times oversampling ($L = 4$) is good enough for estimating the PAPR of continuous OFDM signal [17]. Then, zero padded input symbol sequence $\mathbf{X}$ in (6.1) is IFFTed and the nth element of the resulting discrete time domain OFDM signal is expressed as

$$x_n = \frac{1}{\sqrt{LN}} \sum_{k=0}^{N-1} X_k e^{j\frac{2\pi kn}{LN}},\ 0 \le n \le LN-1. \tag{6.2}$$

Fig. 6.1 shows a block diagram of the SLM scheme using CORR metric in the presence of nonlinear HPA. This scheme generates U alternative symbol sequences $\mathbf{X}^{(u)}$ by componentwisely multiplying each of U different phase sequences to an input symbol sequence $[X_0, X_1, \cdots, X_{N-1}]$. Let $\mathbf{P}^{(u)} = [P_0^{(u)}, P_1^{(u)}, \cdots, P_{N-1}^{(u)}]$ be the uth phase sequence with $P_k^{(u)} = e^{j\phi_k^{(u)}}$, where $\phi_k^{(u)} \in [0, 2\pi)$, $0 \le k \le N-1$, and $0 \le u \le U-1$. It is customary to use $P_k^{(u)} \in \{1, -1\}$ or $P_k^{(u)} \in \{\pm 1, \pm j\}$.

Each alternative symbol sequence is zero padded and LN-point IFFTed to generate $\mathbf{x}^{(u)} = [x_0^{(u)}, x_1^{(u)}, \cdots, x_{LN-1}^{(u)}]$ and it passes through HPA such as solid state power amplifier (SSPA) which is commonly used in mobile communication systems. It is known

that the polynomial model for estimating the real SSPA to calculate the CORR metric is sufficiently accurate and has relatively low computational complexity [40]. The polynomial model is usually expressed as a third order nonlinearity such that the nth element of the output of SSPA can be expressed [41] as

$$y_n^{(u)} \approx \alpha_1 x_n^{(u)} + \alpha_3 x_n^{(u)} |x_n^{(u)}|^2 \tag{6.3}$$

where $x_n^{(u)}$ and $y_n^{(u)}$ are the nth elements of the uth alternative input and output OFDM signal sequences of SSPA, respectively [40]. As the polynomial coefficients in (6.3), $\alpha_1 = 1$ and $\alpha_3 = -0.1769$ are used to match the practical SSPA used in WiMAX [57]. The CORR metric [56] for the uth alternative OFDM signal sequence is obtained as

$$R_{xy}^{(u)} = \sum_{n=0}^{LN-1} x_n^{(u)} y_n^{(u)*} = \alpha_1 \sum_{n=0}^{LN-1} |x_n^{(u)}|^2 + \alpha_3 \sum_{n=0}^{LN-1} |x_n^{(u)}|^4 \tag{6.4}$$

where $(\cdot)^*$ indicates the complex conjugation. Then, this scheme calculates U CORR metrics between the input signal $\mathbf{x}^{(u)}$ and the output signal $\mathbf{y}^{(u)}$ of SSPA. Among U CORR metrics $R_{xy}^{(u)}$, the signal $\mathbf{x}^{(\tilde{u})}$ with the maximum CORR is selected for transmission. Also, the side information $\tilde{u}$ should be transmitted to the receiver.

As an HPA to amplify the selected alternative OFDM signal at the transmitter, Rapp model [56] is used because it is also widely used in mobile communications and more accurate than the polynomial model in (6.3). The output of Rapp model is given as

$$y_n = A(|x_n|) e^{j[\arg(x_n) + \phi(|x_n|)]} \tag{6.5}$$

where x_n is the input to Rapp model and $A(\cdot)$ and $\phi(\cdot)$ denote amplitude to amplitude (AM/AM) and amplitude to phase (AM/PM) conversions of the nonlinear HPA, respectively. Since SSPA is used in this chapter, AM/PM conversion is assumed flat, i.e.,

$\phi(|x_n|) = 0$, and the AM/AM conversion is given as

$$A(|x_n|) = |x_n| \left[1 + \left(\frac{|x_n|}{A_0} \right)^{2p} \right]^{-\frac{1}{2p}} \tag{6.6}$$

where A_0 is the maximum amplifier output and p is the smoothness factor [**?**] with $p = 3.286$ as given in [56].

To determine the operating point of HPA, we use output back-off (OBO) defined by

$$\mathrm{OBO} = 10 \log_{10} \frac{A_0^2}{P_{\mathrm{out}}} \tag{6.7}$$

where P_{out} denotes the average power of OFDM signal at the output of HPA.

6.2.2. BER Performance of SLM Scheme under HPA

The performance of SLM scheme was analyzed in the presence of nonlinear HPA in [58]. First, we review the analysis in [58] as follows. The output of nonlinear HPA can be formulated as

$$y_n = K_0 x_n + d_n, \ 0 \le n \le N - 1 \tag{6.8}$$

where x_n is the input to the nonlinear HPA, d_n is the uncorrelated distortion, and K_0 is the linear scaling factor defined as

$$K_0 = \frac{E\left[x_n y_n^*\right]}{E\left[\left|x_n\right|^2\right]}. \tag{6.9}$$

Also, signal-to-distortion-plus-noise ratio (SDNR) measured at the receiver after FFT is defined as

$$\mathrm{SDNR} = \frac{E[|K_0 X_k|^2]}{E[|D_k + W_k|^2]} \tag{6.10}$$

where $D_k = \mathrm{FFT}\{d_n\}$ and W_k is AWGN at the kth subcarrier. Assume that X_k, D_k, and W_k are mutually uncorrelated. Then, the average BER [58] is calculated as

$$P_b = \frac{4}{\log_2 M} \left(1 - \frac{1}{\sqrt{M}} \right) Q \left(\sqrt{\frac{3}{M-1} \mathrm{SDNR}} \right) \tag{6.11}$$

Table 6.1: Resultant coefficient sequences after computing CORR when L times oversampling is used.

Index	1	2	3	4	5	6	7	8
$L=1$	0	0	0	0	0	1	0	0
$L=2$	0.04	-0.13	-0.13	0.04	-0.13	1.4	0.4	-0.13
$L=4$	0.09	-0.33	-0.3	0.09	-0.33	2.3	0.94	-0.3
$L=16$	0.37	-1.42	-1.25	0.36	-1.42	7.72	3.94	-1.25
Index	9	10	11	12	13	14	15	16
$L=1$	0	0	0	0	0	0	0	0
$L=2$	-0.13	0.4	0.4	-0.13	0.04	-0.13	-0.13	0.04
$L=4$	-0.3	0.94	1.3	-0.33	0.09	-0.3	-0.33	0.09
$L=16$	-1.25	3.94	6.72	-1.42	0.36	-1.25	-1.42	0.37

where M is the constellation order and $Q(\cdot)$ denotes the Q-function.

According to (6.11), to achieve good BER performance, SDNR should be large. That is, the numerator in (6.10) should be large because D_k and W_k cannot be controlled. Since $E[|K_0 X_k|^2] = K_0^2 E[|x_k|^2]$ and $E[|x_k|^2] =$ constant, for good BER performance, $E\left[x_n^{(u)} y_n^{(u)*}\right]$ in (6.9) should be large, which is identical to the CORR metric in (6.4). Therefore, the CORR metric can be regarded as near optimal in terms of BER performance of the SLM scheme for OFDM signals.

From this reason, we will focus on the CORR metric among various metrics targeting the BER performance and analyze the oversampling effect on the SLM scheme using CORR metric in the presence of nonlinear HPA.

6.3. Oversampling Effect on SLM Scheme Using CORR Metric

6.3.1. Expression of Oversampled Signal and CORR Metric

Oversampled signal can be expressed by linear combination of Nyquist-rate samples [16]. The oversampling operator is called interpolator and the impulse response of an interpolator for L times oversampling is defined as

$$h_L[n] = \frac{\sin(\pi n/L)}{\pi n/L}. \tag{6.12}$$

Since an ideal interpolator cannot be implemented, a finite-length filter of length I is used in practice. Then, the output of finite-length interpolator can be expressed as

$$\tilde{x}_L[n_L] = \sum_{k=\lceil (n_L - LI)/L \rceil}^{\lfloor (n_L+LI)/L \rfloor} x[k] h_L[n_L - Lk] \tag{6.13}$$

where $\tilde{x}_L[n_L]$ is the estimated n_Lth element of L times oversampled signal and $x[k]$ denotes the kth element of Nyquist-rate signal. In this chapter, we assume $I = 2$ for simplicity and for $I > 2$, a similar analysis can be applied.

To represent the continuous signal, it is known that 16 times oversampling ($L = 16$) is good enough. By substituting $L = 16$ and $I = 2$ to (6.13), 16 times oversampled signal $\tilde{x}_{16}[16m + s]$ can be obtained as

$$\begin{aligned}\tilde{x}_{16}[16m + s] &= h_{16}[16 + s]x[m - 1] + h_{16}[s]x[m] \\ &\quad + h_{16}[-16 + s]x[m + 1] + h_{16}[-32 + s]x[m + 2].\end{aligned} \tag{6.14}$$

where $0 \leq m \leq N - 1$ denotes the indices of Nyquist-rate samples and $0 \leq s \leq 15$. We can also obtain $\tilde{y}_{16}[16m + s]$ in the similar manner.

Note that the purpose of this analysis is investigating how frequently the same phase sequences are selected when L times oversamplings are used compared to the case of 16 times oversampling. Therefore, we first investigate the result of CORR metric when 16 times oversampling is used and then, compare the result from L times oversampling cases. In order to do this, we only need to consider 16 samples for CORR metric computation in (6.4) instead of total $16N$ samples. Since the same filter coefficients $h_{16}[n]$ in (6.12) are used for all m in (6.14), the resulting coefficients of CORR metric for $16N$ samples is just multiple of resulting coefficients of CORR metric for 16 samples.

Then, a partial CORR metric of 16 samples within two adjacent Nyquist-rate samples can be given as

$$\bar{R}_{\tilde{x}\tilde{y}}^{(u)}(m) = \sum_{s=0}^{15} \tilde{x}_{16}[16m+s]^{(u)} \tilde{y}_{16}[16m+s]^{(u)*} = \sum_{s=0}^{15} v_m(s). \tag{6.15}$$

For better understanding, we can rewrite $v_m(8)$ by substituting (6.14) and $s = 8$ to

(6.15) as

$$
\begin{aligned}
v_m(8) &= \tilde{x}_{16}[16m+8]^{(u)}\tilde{y}^*_{16}[16m+8]^{(u)} \\
&= (-0.21x[m-1]^{(u)} + 0.63x[m]^{(u)} + 0.63x[m+1]^{(u)} - 0.21x[m+2]^{(u)}) \\
&\quad (-0.21y[m-1]^{(u)} + 0.63y[m]^{(u)} + 0.63y[m+1]^{(u)} - 0.21y[m+2]^{(u)})^* \\
&= 0.04x[m-1]^{(u)}y^*[m-1]^{(u)} - 0.13x[m-1]^{(u)}y^*[m]^{(u)} \\
&\quad - 0.13x[m-1]^{(u)}y^*[m+1]^{(u)} + 0.04x[m-1]^{(u)}y^*[m+2]^{(u)} \\
&\quad - 0.13x[m]^{(u)}y^*[m-1]^{(u)} + 0.4x[m]^{(u)}y^*[m]^{(u)} \\
&\quad + 0.4x[m]^{(u)}y^*[m+1]^{(u)} - 0.13x[m]^{(u)}y^*[m+2]^{(u)} \\
&\quad - 0.13x[m+1]^{(u)}y^*[m-1]^{(u)} + 0.4x[m+1]^{(u)}y^*[m]^{(u)} \\
&\quad + 0.4x[m+1]^{(u)}y^*[m+1]^{(u)} - 0.13x[m+1]^{(u)}y^*[m+2]^{(u)} \\
&\quad + 0.04x[m+2]^{(u)}y^*[m-1]^{(u)} - 0.13x[m+2]^{(u)}y^*[m]^{(u)} \\
&\quad - 0.13x[m+2]^{(u)}y^*[m+1]^{(u)} + 0.04x[m+2]^{(u)}y^*[m+2]^{(u)}. \qquad (6.16)
\end{aligned}
$$

All the other values $v_m(s)$ can be derived similarly. Note that in (6.16), there are 16 coefficients, i.e., $\{0.04, -0.13, -0.13, \cdots, -0.13, 0.04\}$ and we will call the coefficient set as a coefficient sequence.

Now, suppose that arbitrary $L \in \{1, 2, 4, 16\}$ times oversamplings are used for CORR metric computation. Then, from (6.4), we only need $v_m(0)$ in (6.15) for Nyquist-rate sampling. Also, note that $v_m(0) + v_m(8)$, $v_m(0) + v_m(4) + v_m(8) + v_m(12)$, and $\sum_{s=0}^{15} v_m(s)$ are needed to compute $\bar{R}^{(u)}_{\tilde{x}\tilde{y}}(m)$ in (6.15) when two times, four times, and 16 times oversamplings are used, respectively.

6.3.2. Correlation Coefficients between Coefficient Sequences Derived from CORR Metric Computation

In this subsection, we will investigate oversampling rate required to show the similar performance as the continuous OFDM signal case. Note that BER performance of SLM scheme using CORR metric is determined by the selected phase sequence $\mathbf{P}^{(\tilde{u})}$. Therefore, to find the proper oversampling rate, we have to investigate which oversampling case selects the same phase sequences as the continuous OFDM signal case, i.e., 16 times oversampling case. Since the selection of phase sequences is determined by (6.15) for all m, we need the resultant coefficient sequences after computing (6.15) when $L \in \{1, 2, 4, 16\}$. Then, by investigating the correlation coefficients of the resultant coefficient sequences, we can find the proper oversampling rate.

Table 6.1 shows the resultant coefficient sequences after computing (6.15) when $L = 1, 2, 4$, and 16. Note that indices are arranged from left to right and top to bottom (1 to 16) in a coefficient sequence as given in (6.16). For example, when $L = 2$, we need $v_m(0) + v_m(8)$ to compute (6.15). Since $v_m(0) = \tilde{x}_{16}[16m]^{(u)}\tilde{y}_{16}[16m]^{(u)*} = 1 \cdot x[m]^{(u)}y[m]^{(u)*}$, there is only one nonzero coefficient 1 at index 6. Therefore, the coefficient 1 should be added to 0.4 at index 6 in $v_m(8)$, i.e., $1 + 0.4 = 1.4$ (see Table 6.1 when $L = 2$ and (6.16)). The rests can also be computed in the same manner.

Now, we want to investigate the similarity between coefficient sequences in $\{v_m(0), v_m(0) + v_m(8), v_m(0) + v_m(4) + v_m(8) + v_m(12), \sum_{s=0}^{15} v_m(s)\}$. In this chapter, we use the Pearson correlation coefficient r because it is a measure of correlation between two sequences. The Pearson correlation coefficient between two sequences $\mathbf{a}$ and $\mathbf{b}$ is

Table 6.2: Values of Pearson correlation coefficients between coefficient sequences with different L.

	$L = 1$ and $L = 16$	$L = 2$ and $L = 16$	$L = 4$ and $L = 16$
r	0.6023	0.9133	0.9839

defined as

$$r = \frac{\sum_i (a_i - \bar{\mathbf{a}})(b_i - \bar{\mathbf{b}})}{\sqrt{\sum_i (a_i - \bar{\mathbf{a}})^2 \sum_i (b_i - \bar{\mathbf{b}})^2}} \tag{6.17}$$

where $\bar{\mathbf{a}}$ denotes the sample mean of $\mathbf{a}$ and a_i denotes the ith elements of the sequence $\mathbf{a}$. Clearly, r takes a value in $[-1, 1]$, where 0 implies no correlation and 1 or -1 implies positive or negative correlation, respectively.

Table 6.2 shows r between two coefficient sequences obtained from Table 6.1 when different L's are used. When the cases of $L = 1$ and $L = 16$ are considered, the value of r is 0.6023, which shows relatively low correlation. On the other hand, when the cases of $L = 2$ and $L = 16$ and the cases of $L = 4$ and $L = 16$ are considered, the values of r are 0.9133 and 0.9839, respectively, which show relatively high correlation. These results imply that when two times or four times oversamplings are used, the probability of choosing the same phase sequences as the 16 times oversampling case in the SLM scheme using CORR metric is very high.

Table 6.3 shows the probabilities of choosing different phase sequences from 16 times oversampling case for various values of L when $N = 256$. 10^4 OFDM signals are randomly generated and the unequal cases are counted. When $L = 1$ and $U = 4$, the probability is 0.343 and it increases as U increases. However, when $L = 2$ and 4, the probabilities are all zero. That is, they always choose the same phase sequence as the

Table 6.3: Probability of choosing different phase sequences compared with 16 times oversampling case when $N = 256$.

	$U = 4$	$U = 8$	$U = 16$	$U = 32$
$L = 1$	0.343	0.443	0.501	0.604
$L = 2$	0	0	0	0
$L = 4$	0	0	0	0

case of $L = 16$. This result confirms that analysis using Pearson correlation coefficient is reasonable.

6.4. Computational Complexity

In this section, computation complexity of original CORR SLM scheme with four and two times oversampling cases are compared. Only the metric calculation in (6.4) is considered because the rests are all the same. Also, real multiplication (RM) and real addition (RA) are considered. For original (four times oversampling case) CORR SLM scheme, $3LN + 1$ RMs and $3LN = 1$ RAs are required. Whereas, for the proposed scheme (two times oversampling case), $3LN/2 + 1$ RMs and $LN - 1$ RAs are required.

Computational complexity of CORR SLM scheme is compared in Table 6.4 when $N = 256$ and 1024. The computational complexity reductio ratio (CCRR) is defined as

$$\text{CCRR} = \left(1 - \frac{\text{Complexity of the proposed scheme}}{\text{Complexity of original scheme}}\right) \times 100(\%). \tag{6.18}$$

For RM, CCRR is 49.98% and 49.99% when $N = 256$ and 1024, respectively. For RA, CCRR is 66.68% and 66.67% when $N = 256$ and 1024, respectively.

Table 6.4: Comparison of computational complexity required for metric computation of CORR SLM scheme when $N = 256$ and 1024.

	Original ($N = 256$)	Proposed ($N = 256$)
RM	3,073	1,537
RA	3,071	1,023
	Original ($N = 1024$)	Proposed ($N = 1024$)
RM	12,289	6,145
RA	12,287	4,095

6.5. Simulation Results

In this section, the BER performances of the SLM scheme using CORR metric for different oversampling factor L are compared when $N = 256$, $U = 4$, and OBO $= 3, 3.5, 4, 4.5$, and 5 dB. A_0 in (6.7) is calculated by multiple simulations for a given OBO. We only consider the AWGN channel since the BER performance of the SLM scheme using CORR in selective fading channel is shown in [56]. For simulation, nonlinear HPA is used and 16 times oversampling is used for Rapp model to estimate the performance of continuous OFDM signal case. We assume the perfect knowledge of side information.

In Fig. 6.2, Original, CL, and No HPA indicate the original OFDM signal with nonlinear HPA, OFDM signal using CORR metric under nonlinear HPA where L denotes the oversampling factor for computing CORR metrics in (6.4), and the original OFDM signal without nonlinear HPA, respectively. Note that C2, C4, and C16 show almost the

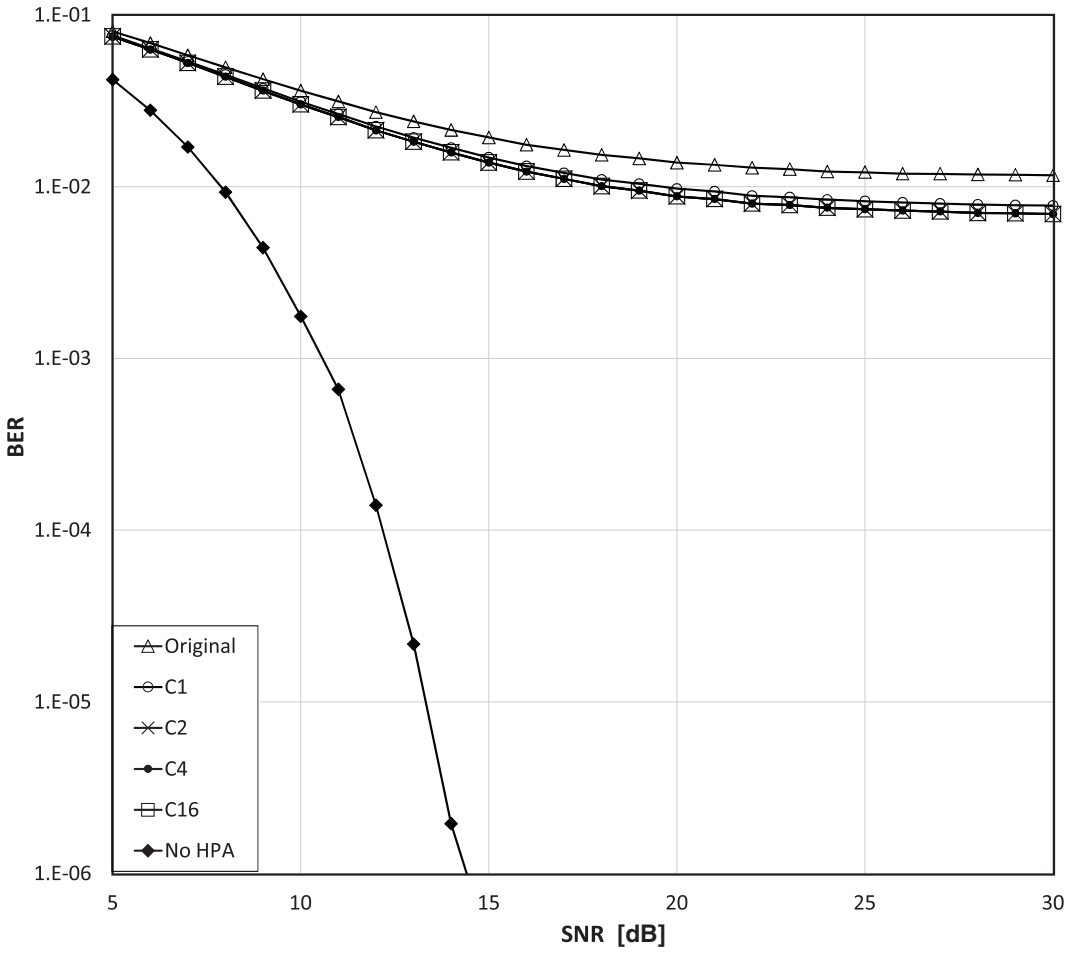
1.E-01
1.E-02
1.E-03
1.E-04
1.E-05
1.E-06
BER
5
10
15
20
25
30
SNR [dB]
Original
C1
C2
C4
C16
No HPA

(a)

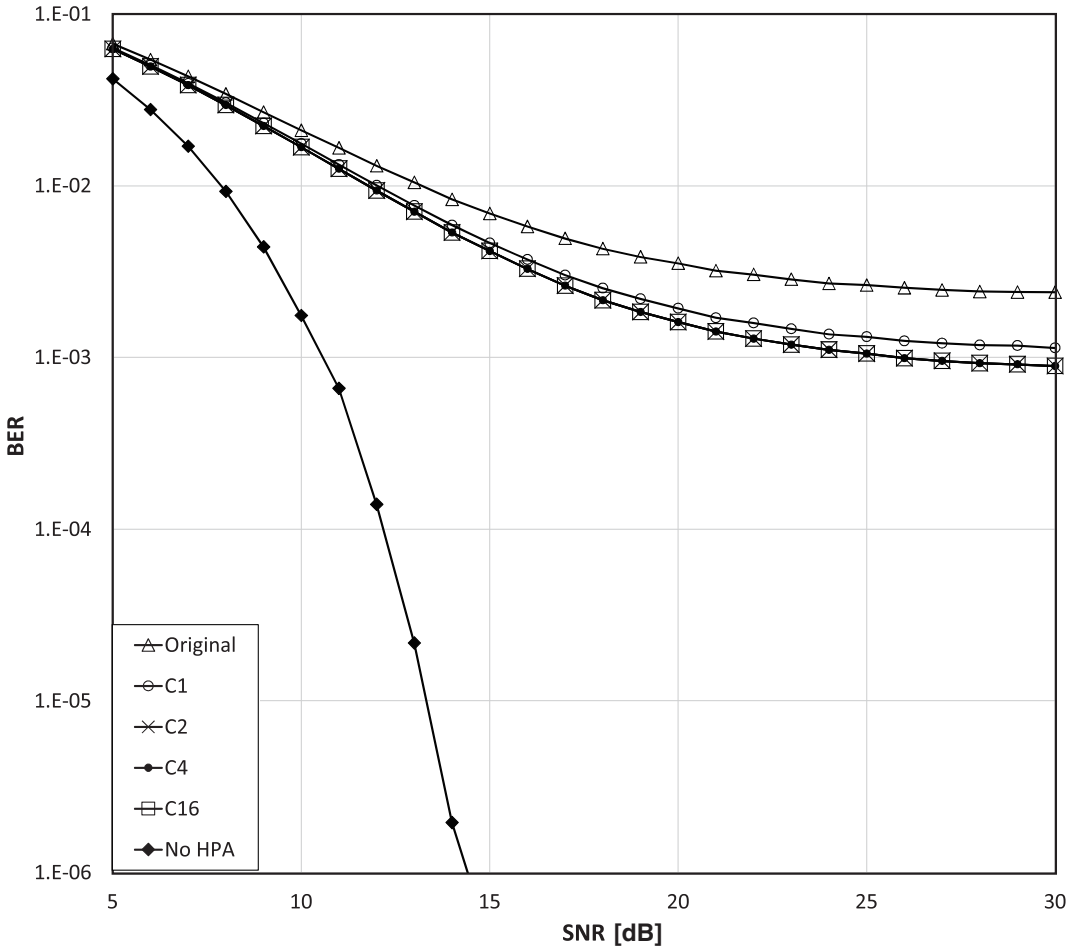
1.E-01
1.E-02
1.E-03
1.E-04
1.E-05
1.E-06
BER
5
10
15
20
25
30
SNR [dB]
Original
C1
C2
C4
C16
No HPA

(b)

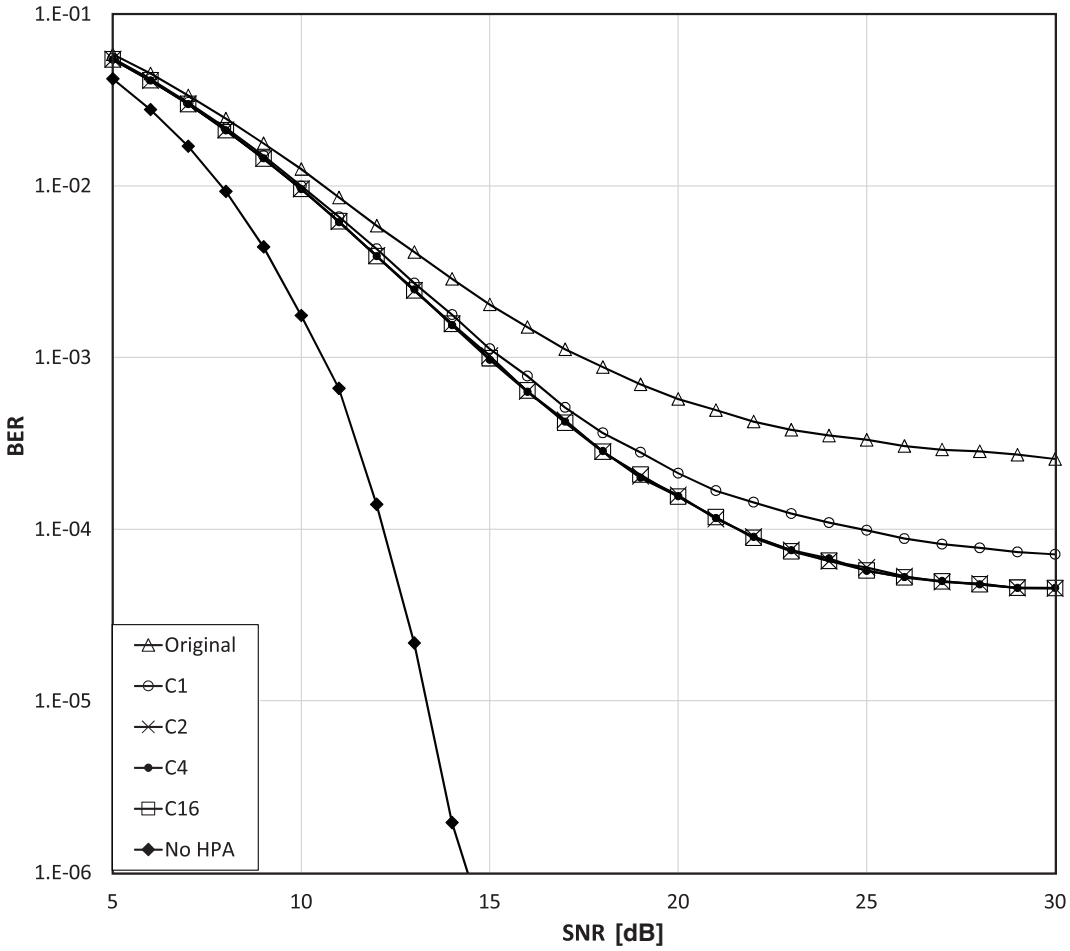
1.E-01
1.E-02
1.E-03
1.E-04
1.E-05
1.E-06
BER
5
10
15
20
25
30
SNR [dB]
Original
C1
C2
C4
C16
No HPA

(c)

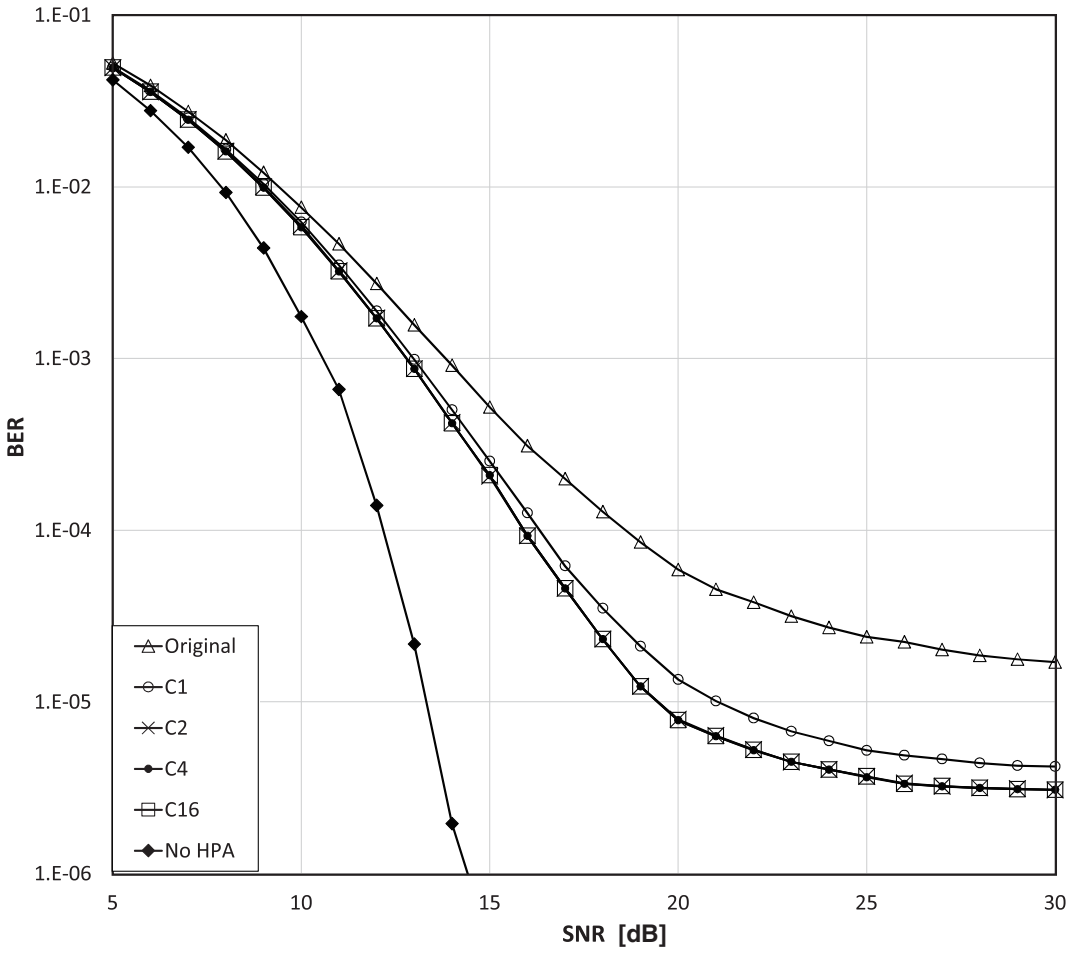
1.E-01
1.E-02
1.E-03
1.E-04
1.E-05
1.E-06
BER
5
10
15
20
25
30
SNR [dB]
Original
C1
C2
C4
C16
No HPA

(d)

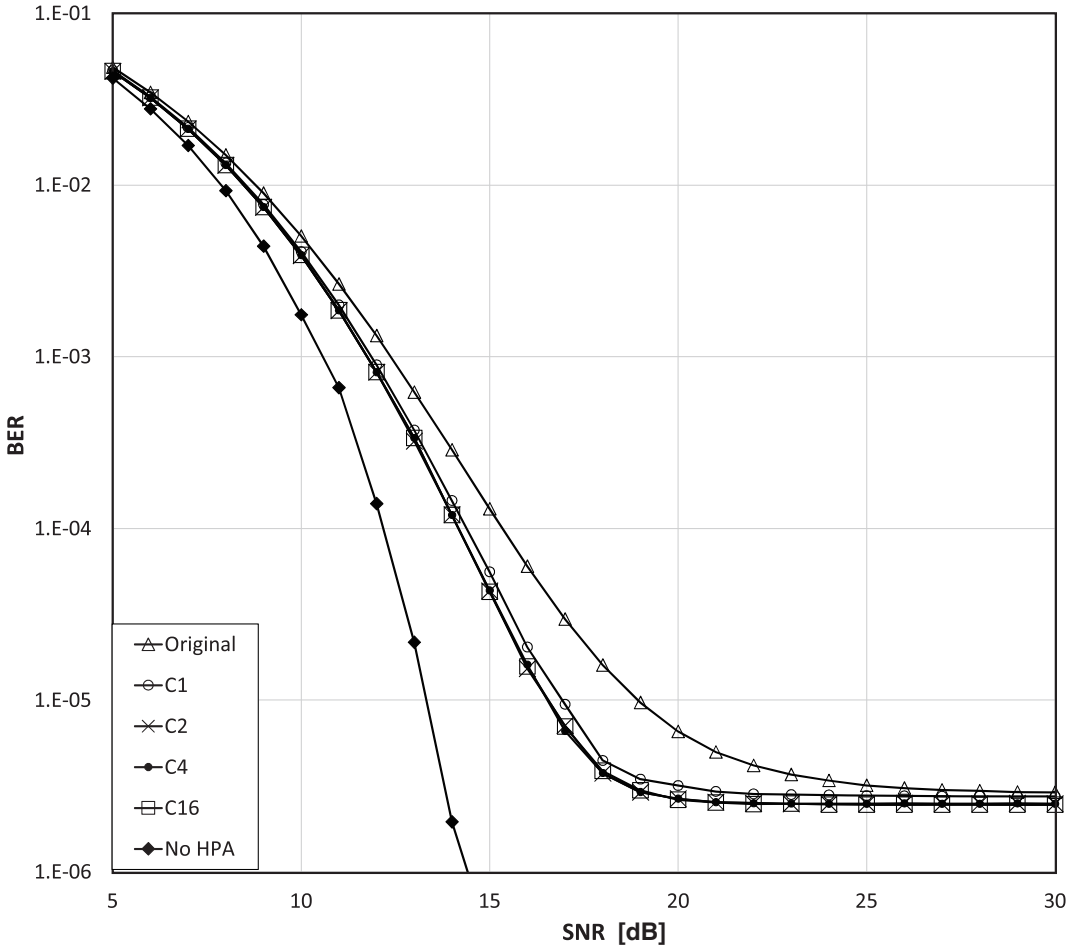

(e)

Figure 6.2: BER performance of the SLM schemes using CORR metric when $N = 256$, $U = 4$, and $L = 1, 2, 4$, and 16 for various OBOs: (a) 3 dB, (b) 3.5 dB, (c) 4 dB, (d) 4.5 dB, and (e) 5 dB.

same BER performances for various OBO values, while C1 is degraded compared to them.

6.6. Discussions

Two different types of HPA are used in CORR SLM scheme: (a) Polynomial model and (b) Rapp model. Polynomial model is used only for CORR computation. That is, the selected phase sequence by CORR computation is determined by polynomial model, whereas, Rapp model is used for amplifying the transmitted signal. Note that same polynomial model is applied to all alternative OFDM signal sequences to compute CORR.

In this section, two subjects are discussed. First, the effect of α_3 on BER performance is discussed. Second, the modified CORR metrics are proposed to reduce the computational complexity.

6.6.1. Effect of α_3

In this section, the effect of α_3 in (6.3) is discussed. $\alpha_3 = -0.1769$ is considered in this study. However, other values of $\alpha_3 = -0.1769$ are also considered for comparison such as -0.147 and -0.207.

Fig. 6.3 shows the magnitude characteristic of polynomial model with various values of α_3. Actually, there is no huge difference in magnitude characteristics for different α_3. When $\alpha_3 = -0.207$, the linear region of HPA is the narrowest. If input magnitude is larger than 1.5, the output magnitude of polynomial model with $\alpha_3 = -0.207$ will be highly distorted.

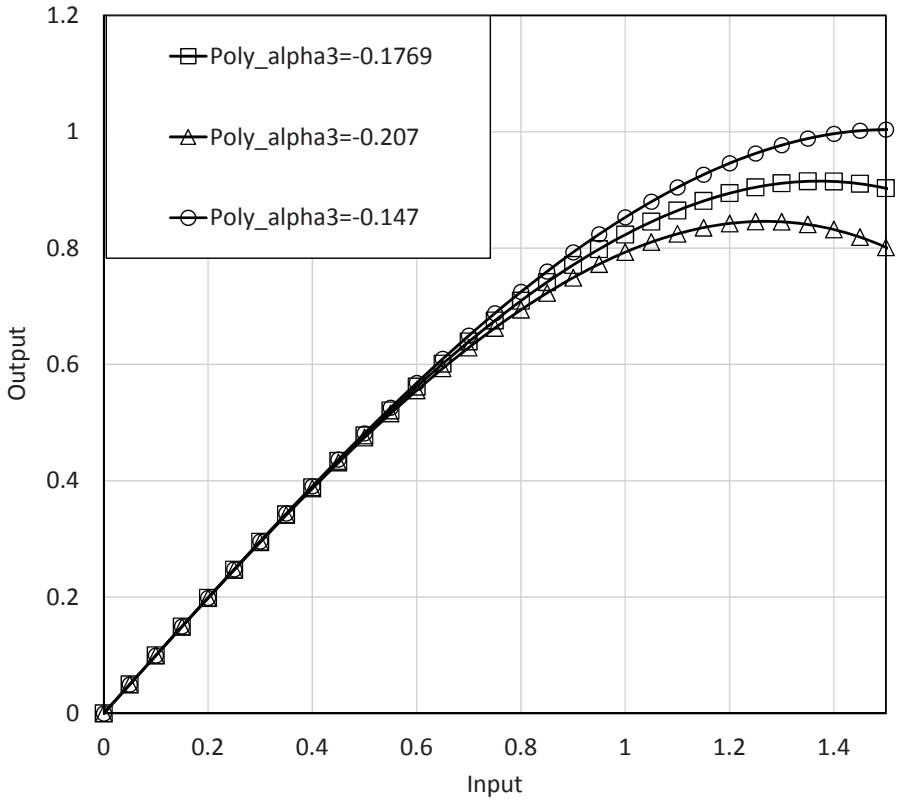

Figure 6.3: Magnitude characteristic of polynomial model with various values of α_3.

Fig. 6.4 shows the BER performance of CORR SLM scheme for various values of L and α_3. In Fig. 6.4, three values of α_3 are used. C2 and C4 show almost the same BER performance for all cases. Whereas, C1 shows performance degradation. There is only slight difference of BER performance with different α_3's. That is, the effect of α_3 is negligible in CORR SLM scheme.

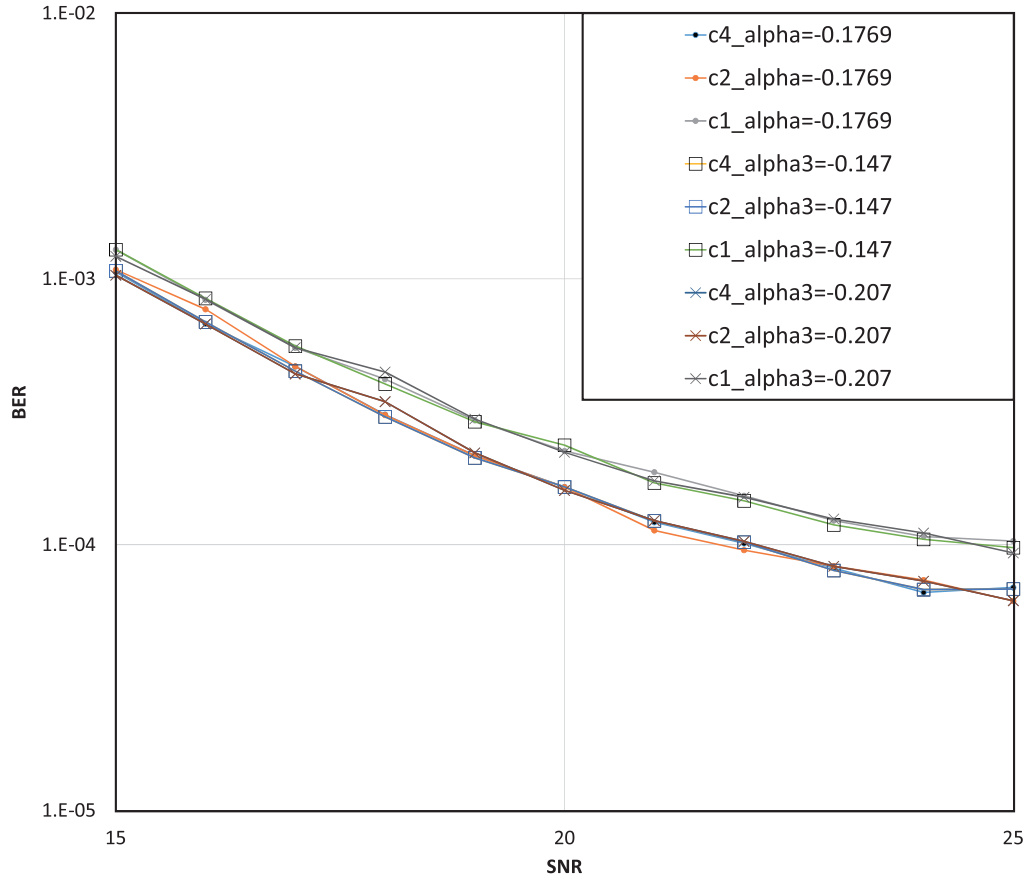

Figure 6.4: BER performance of CORR SLM scheme with various values of L and α_3.

6.6.2. Future Work

In this section, two modified CORR metrics are discussed. One is using LN samples for CORR computation. However, the computational complexity for computing CORR of one sample can be reduced. The other one is reducing the number of samples for CORR computation.

Table 6.5: Computational complexity of C-CORR when $N = 256$ and 1024 and the corresponding CCRR.

	$N = 256$	$N = 1024$
RM	2,048	8,192
RA	2,047	8,191
CCRR (%)	33.42	33.35

6.6.2.1. Comparative CORR

LN samples of alternative OFDM signal sequences are used for CORR computation in (6.4). Since the power of OFDM signal sequence is constant for all alternative OFDM signal sequences, CORR (6.4) can be reduced to

$$\mathrm{R-CORR} = \alpha_3 \sum_{n=0}^{LN-1} |x_n^{(u)}|^4. \tag{6.19}$$

By using R-CORR instead of CORR, the computational complexity can be reduced. Also, it is shown that two times oversampling can be used instead of four times oversampling. Since the half size of IFFT is used, the computational complexity is reduced.

Can we further reduce the computational complexity for CORR SLM scheme? To do this, comparative-CORR (C-CORR) is proposed as

$$\mathrm{C-CORR} = \sum_{n=0}^{LN-1} \max\left(|a_n^{(u)}|,\ |b_n^{(u)}|\right)^4 \tag{6.20}$$

where $x_n^{(u)} = a_n^{(u)} + jb_n^{(u)}$. That is, only the maximum of real and imaginary parts is computed for CORR. The required RM and RA are $2N$ and $2N - 1$, respectively.

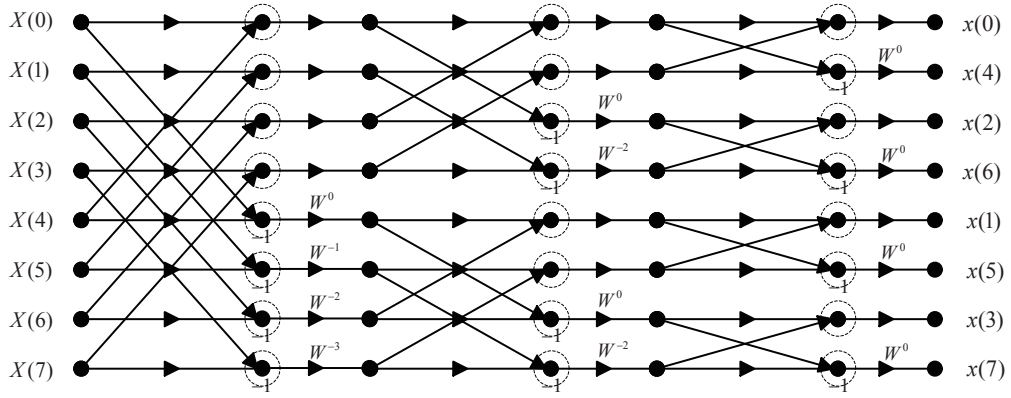

Figure 6.5: A block diagram of 8-point decimation in time IFFT structure.

Table 6.5 shows the computational complexity of C-CORR. When $N = 256$, RM and RA are 512 and 511, respectively and CCRR is 33.42. Also, when $N = 1024$, RM and RA are 2,048 and 2,047, respectively and CCRR is 33.35. CCRR decreases as N increases.

6.6.2.2. Low Sampled CORR

To reduce the number of samples for CORR computation, IFFT structure is used. Fig. 6.5 shows decimation in time 8-point IFFT structure. Assume that four time domain samples are used in Fig. 6.5. Then, $1/2$ part of total IFFT structure is required approximately. Based on this result, low sampled CORR (LS-CORR) is proposed as

$$\mathrm{LS{-}CORR} = \sum_{m=0}^{LN/2-1} |x_m^{(u)}|^4 \tag{6.21}$$

where $m = \{n | n \bmod 2 = 0,\ n = 0, \cdots, LN-1\}$. In addition to this, $n \bmod 4 = 0$ or $n \bmod 8 = 0$ cases are possible. Then, $1/4$ or $1/8$ of total IFFT structure is required, respectively. However, BER is increased as the number of samples decreases.

Table 6.6: Computational complexity of LS-CORR ($N/2$ samples) when $N = 256$ and 1024 and the corresponding CCRR.

	$N = 256$	$N = 1024$
RM	1,536	6,144
RA	1,023	4,095
CCRR (%)	50	66.67

The required RM and RA of LS-CORR is $3N/2$ and $N - 1$, respectively. The computational complexity of LS-CORR with $N/2$ samples is shown in Table 6.6.

6.7. Conclusions

In this chapter, the oversampling effect for the SLM scheme using CORR metric is analyzed in the presence of nonlinear HPA. The oversampled signals for CORR metric computation for $L = 1, 2, 4,$ and 16 are obtained by linear combination of Nyquist-rate samples. As a result, two and four times oversampling cases show relatively high correlation with 16 times oversampling case, but Nyquist-rate sampling case shows relatively low correlation with 16 times oversampling case. These results imply that, when two times oversampling is used for CORR metric computation, the probability of choosing the same phase sequence as the 16 times oversampling case is very high.

Simulation results show that BER performance of two times oversampling for CORR metric calculation is almost the same as that of four or 16 times oversampling cases. On the other hand, the BER performance for Nyquist-rate sampling case is degraded.

Consequently, two times oversampling for CORR metric computation is good enough to achieve the same BER performance as those of the four or 16 times oversampling case in the SLM scheme. By using two times oversampling instead of four to compute CORR, the size of IFFT is reduced to half. Also, the number of samples in (6.4) is reduced half. As a result, CCRR of RM and RA when two times oversampling is used for CORR computation is both 50% approximately.

Chapter 7. Conclusions

In this study, low-complexity schemes for Class-III and CORR SLM schemes in OFDM systems are proposed. The objective of Class-III SLM scheme is reducing the PAPR of OFDM signal sequences, while that of CORR SLM scheme is reducing BER of OFDM signal sequences.

In Chapter 5, a selection method of the optimal cyclic shift values for Class-III SLM scheme is proposed. Also, a selection method of good additional alternative OFDM signal sequences by using proper rotation values is proposed. $N/8$ alternative OFDM signal sequences satisfying the optimal condition in Section 5.3.2 by using the optimal cyclic shift values in Table 5.2 when $U < N/8$. Note that this method does not require the rotation values. To generate more than $N/8$ alternative OFDM signal sequences, rotation values which do not have linear relation are used.

To use the proposed scheme, we only need U pre-determined optimal cyclic shift values given in Table 5.2.

There are some advantages of the proposed scheme. First, the random scheme requires memory for 3 complex numbers (rotation values), whereas the proposed scheme does not need the memory for rotation values. Second, the random scheme requires $\lceil \log_2 (N/4)^3 \rceil$ bits of side information for cyclic shift values and $\lceil \log_2 4^3 \rceil$ bits of side information for rotation values. Whereas, the proposed scheme requires only $\lceil \log_2 U \rceil$

bits of side information if the cyclic shift values in Table 5.2 are shared by transmitter and receiver. Note that the side information for the proposed scheme is a function of U. Whereas, that of the random scheme is a function of N. Since $N \gg U$, that of the random scheme is much larger than the proposed scheme. Third, the random scheme has a risk to select the cases of bad PAPR reduction performance, whereas the proposed scheme always guarantees the optimal PAPR reduction performance in terms of minimizing VC.

In Chapter 6, the oversampling effect for the SLM scheme using CORR metric is analyzed in the presence of nonlinear HPA. The oversampled signals for CORR metric computation for $L = 1, 2, 4,$ and 16 are obtained by linear combination of Nyquist-rate samples. As a result, two and four times oversampling cases show relatively high correlation with 16 times oversampling case, but Nyquist-rate sampling case shows relatively low correlation with 16 times oversampling case. These results imply that, when two times oversampling is used for CORR metric computation, the probability of choosing the same phase sequence as the 16 times oversampling case is very high.

Simulation results show that BER performance of two times oversampling for CORR metric calculation is almost the same as that of four or 16 times oversampling cases. On the other hand, the BER performance for Nyquist-rate sampling case is degraded.

Consequently, two times oversampling for CORR metric computation is good enough to achieve the same BER performance as those of the four or 16 times oversampling case in the SLM scheme. By using two times oversampling for CORR metric computation, the computational complexity can be reduced to $1/2$ as that of the four times oversampling case.

Bibliography

[1] R. W. Chang and R. A. Gibby, "A theoretical study of performance of an orthogonal multiplexing data transmission scheme," *IEEE Trans. Commun.*, vol. COM-16, no. 4, Aug. 1968.

[2] "Radio broadcasting system: Digital audio broadcasting (DAB) to mobile, portable and fixed receivers," *ETSI*, ETS 300 410, 1.3.2 ed., 2000.

[3] "Digital video broadcasting(DVB): Framing structure, channel coding and modulation for digital terrestrial television," *ETSI*, EN 300 744, 1.3.1 ed., 2000.

[4] IEEE Part 11: Wireless LAN medium access control (MAC) and physical layer (PHY) specifications: High-speed physical layer in the 5 GHz band, *IEEE Std*. 802. 11a-1999, Sep. 1999.

[5] S. B. Weinstein and P. M. Erbert, "Data transmission by frequency-division multiplexing using the discrete Fourier transform," *IEEE Trans. Commun.*, vol. COM-19, pp. 628–634, Oct. 1971.

[6] A. Peled and A.Ruiz, "Frequency domain data transmission using reduced computational complexity algorithms," in *Proc. IEEE ICASSP,* vol. 5, Apr. 1980, pp. 964–967.

[7] R. van. Nee and R. Prasad, *OFDM for Wireless Multimedia Communications*, Boston, MA: Artech House, 1999.

[8] A. V. Oppenheim and R. W. Schafer, *Discrete-Time Signal Processing, 2nd Ed.* Upper Saddle River, NJ: Prentice Hall, 1998.

[9] J. Armstrong, "Analysis of new and existing methods of reducing intercarrier interference due to carrier frequency offset in OFDM," *IEEE Trans. Commun.,* vol. 47, pp. 365–369, Mar. 1999.

[10] Y. Zhao and S. Häggman, "Intercarrier interference self-cancellation scheme for OFDM mobile communication systems," *IEEE Trans. Commun.,* vol. 49, pp. 1185-–1191, Jul. 2001.

[11] H. Ochiai and H. Imai, "On the distribution of the peak-to-average power ratio in OFDM signals," *IEEE Trans. Commun.,* vol. 49, no. 5. pp. 282–289, Feb. 2001.

[12] S. H. Müller, R. W. Bäuml, R. F. H. Fischer, and J. B. Huber, "OFDM with reduced peak-to-average power ratio by multiple signal representation," *Ann. Telecommun.*, vol. 52, no.1–2, pp. 58–67, Feb. 1997.

[13] D.-W. Lim, S.-J. Heo, and J.-S. No, "On the phase sequence set of SLM OFDM scheme for a crest factor reduction," *IEEE Trans. Signal Process.*, vol. 54, no. 5, pp. 1931–1935, May 2006.

[14] G. Tong Zhou and Liang Peng, "Optimality condition for selected mapping in OFDM," *IEEE Trans. Signal Processing*, vol. 54, no. 8, pp. 3159–3165, Aug. 2006.

[15] S. J. Heo, H. S. Joo, J. S. No, D. W. Lim, and D. J. Shin, "Analysis of PAPR reduction performance of SLM schemes with correlated phase vectors," *in Proc. IEEE ISIT*, pp.1540–1543, 2009.

[16] C. L. Wang, S. J. Ku, and C. J. Yang, "A low-complexity PAPR estimation scheme for OFDM signals and its application to SLM-based PAPR reduction," *IEEE J. Sel. Topics Signal Process.,* vol. 4, no. 3, pp. 637–645, Jun. 2010.

[17] C. Tellambura, "Computation of the continuous-time PAR of an OFDM signal with BPSK subcarriers," *IEEE Commun. Lett.,* vol. 5, no. 5, pp. 185–187, May 2001.

[18] G. Wunder and H. Boche, "Peak value estimation of bandlimited signals from their samples, noise enhancement, and a local characterization in the neighborhood of an extremum," *IEEE Trans. Signal Process.,* vol. 51, no. 3, pp. 771–780, Mar. 2003.

[19] S. Litsyn and A. Yudin, "Discrete and continuous maxima in multicarrier communication," *IEEE Trans. Inf. Theory*, vol. 51, no. 3, pp. 919–928, Mar. 2005

[20] S. Le Goff, B. Khoo, C. Tsimenidis, and B. Sharif, "A novel selected mapping technique for PAPR reduction in OFDM systems," *IEEE Trans. Commun.,* vol. 56, no. 11, pp. 1775–1779, Nov. 2008.

[21] T. Jiang and Y. Wu, "An overview: Peak-to-average power ratio reduction techniques for OFDM signals," *IEEE Trans. Broadcast.*, vol. 54, no. 2, pp. 257–268, Jun. 2008.

[22] D. W. Lim, S. J. Heo, and J. S. No, "An Overview of Peak-to-Average Power Ratio Reduction Schemes for OFDM Signals," *J. Commun. Netw.*, vol. 11, no. 3, pp. 229–239, Jun. 2009.

[23] X. Li and L. J. Cimini, "Effects of clipping and filtering on the performance of OFDM," *IEEE Commun. Lett.,* vol.2, no. 5. pp. 131–133, May 1998.

[24] J. Armstrong, "Peak-to-average power reduction for OFDM by repeated clipping and frequency domain filtering," *Elect. Lett.*, vol. 38, no. 8, pp. 246–47, Feb. 2002.

[25] J. Tellado and J. M. Cioffi, "PAR reduction in multicarrier transmission systems," *ANSI Document, T1E1.4 TechnicalSubcommottee*, no. 97–367, pp. 1–14, Dec. 8, 1997.

[26] S. Boyd and L. Vandenberghe, "Lecture notes for introduction to convex optimization with engineering applications," Electrical Engineering Department, Stanford University, CA, 1997.

[27] J. Tellado and J. M. Cioffi, *Multicarrier Modulation with Low PAR, Apprication to DSL and Wireless*. Boston, MA: Kluwer Academic Publisher, 2000.

[28] L. J. Cimini and N. R. Sollenberger, "Peak-to-average power ratio reduction of an OFDM signal using partial transmit sequences," *IEEE Commun. Lett.,* vol. 4, pp. 511–515, Mar. 1999.

[29] D.-W. Lim, J.-S. No, C.-W. Lim, and H. Chung, "A new SLM OFDM scheme with low complexity for PAPR reduction," *IEEE Signal Process. Lett.,* vol. 12, no. 2, pp. 93–96, Feb. 2005.

[30] S. J. Heo, H. S. Noh, J. S. No, and D. J. Shin, "A modified SLM scheme with low complexity for PAPR reduction of OFDM systems," *IEEE Trans. Broadcast.,* vol. 53, no. 4, pp. 804–808, Dec. 2007.

[31] C. L. Wang and Y. Ouyang, "Low-complexity selected mapping schemes for peak-to-average power ratio reduction in OFDM systems," *IEEE Trans. Signal Processing*, vol. 53, no. 12, pp. 4652–4660, Dec. 2005.

[32] D. Lim, S. Heo, J. No, and H. Chung, "A new PTS OFDM scheme with low complexity for PAPR reduction," *IEEE Trans. Broadcast.,* vol. 52, no. 1, pp. 77–82, Mar. 2006.

[33] A. Ghassemi and T. Gulliver, "Partial selective mapping OFDM with low-complexity IFFTs," *IEEE Commun. Lett.,* vol. 12, no. 1, pp. 4–6, Jan. 2008.

[34] R. Baxley and G. Zhou, "Comparing selected mapping and partial transmit sequence for PAR reduction," *IEEE Trans. Broadcast.,* vol. 53, no. 4, pp. 797–803, Dec. 2007.

[35] B. S. Krongold and D. L. Jones, "PAR reduction in OFDM via active constellation extension," *IEEE Trans. Broadcast.,* vol. 49, no. 3, pp. 258–265, Sep. 2003.

[36] K. Sathananthan and C. Tellambura, "Partial transmit sequence and selected mapping schemes to reduce ICI in OFDM systems," *IEEE Commun. Lett.,* vol. 6, no. 8, pp. 313–315, Aug. 2002.

[37] Y. Zhao and S. Häggman, "BER analysis of OFDM communication systems with intercarrier interference," in *Proc. Int. Conf. Commun. Technol.,* Beijing, China, Oct. 1998.

[38] M. R. D. Rodrigues and I. J. Wassell, "IMD reduction with SLM and PTS to improve the error-probability performance of nonlinearly distorted OFDM signals," *IEEE Trans. Veh. Technol.,* vol. 55, no. 2, pp. 537–548, Mar. 2006.

[39] D. Park and H. Song, "A new PAPR reduction technique of OFDM system with nonlinear high power amplifier," *IEEE Trans. Consum. Electron.,* vol. 53, no. 2, pp. 327–332, May 2007.

[40] E. Al-Dalakta, A. Al-Dweik, A. Hazmi, C. Tsimenidis, and B. Sharif, "Efficient BER reduction technique for nonlinear OFDM transmission using distortion prediction," *IEEE Trans. Veh. Technol.*, vol. 61, no. 5, pp. 2330–2336, Jun. 2012.

[41] V. Bohara and S. H. Ting, "Theoretical analysis of OFDM signals in nonlinear polynomial models," in *Proc. IEEE Int. Conf. Inf. Commun. Signal Process.,* 2007, pp. 1–5.

[42] A. Behravan and T. Eriksson, "PAPR and other measures for OFDM systems with nonlinearity," in *Proc. Int. Symp. Wireless Pers. Multimedia Commun.,* 2002, pp. 149–153.

[43] J. A. Davis and J. Jedwab, "Peak-to-mean power control in OFDM, Golay complementary sequences, and Reed.Muller codes," *IEEE Trans. Inf. Theory,* vol. 45, no. 7, pp. 2397-–2417, Nov. 1999.

[44] M. Sharif and B. Hassibi, "Existence of codes with constant PMEPR and related design," *IEEE Trans. Signal Process.,* vol. 52, no. 10, pp. 2836–2846, Oct. 2004.

[45] S. Litsyn and A. Shpunt, "A balancing method for PMEPR reduction in OFDM signals," *IEEE Trans. Commun.,* vol. 55, no. 4, pp. 683–691, Apr. 2007.

[46] Y. C. Tsai, S. K. Deng, K. C. Chen, and M. C. Lin, "Turbo coded OFDM for reducing PAPR and error rates," *IEEE Trans. Wireless Commun.,* vol. 7, no. 1, pp. 84-–89, Jan. 2008.

[47] O. Daoud and O. Alani, "Reducing the PAPR by utilisation of the LDPC code," *IET Commun.*, vol. 3, no. 4, pp. 520—529, Apr. 2009.

[48] M. Sharif, V. Tarokh, and B. Hassibi, "Peak power reduction of OFDM signals with sign adjustment," *IEEE Trans. Commun.,* vol. 57, no. 7, pp. 2160–2166, Jul. 2009.

[49] A. D. S. Jayalath and C. Tellambura, "Adaptive PTS approach for reduction of peak-to-average power ratio of OFDM signal," *Electron. Lett.,* vol. 36, no. 14, pp. 1226–1228, Jul. 2000.

[50] W. Henkel and V. Azis, "Partial transmit sequences and trellis shaping," in *Proc. 5th Int. ITG Conf. Source and Channel Coding (SCC)*, Erlangen, Germany, Jan. 14–16, 2004.

[51] W. Henkel and V. Zrno, "PAR reduction revisited: An extension to Tellado's method," in *Proc. 6th Int. OFDM Workshop,* Sep. 18–19, 2001, pp. 31-1–31-6.

[52] C. L. Wang and S. J. Ku, "Novel conversion matrices for simplifying the IFFT computation of an SLM-based PAPR reduction scheme for OFDM systems," *IEEE Trans. Commun.*, vol. 57, no. 7, pp. 1903–1907, Jul. 2009.

[53] P. Cheng, Y. Xiao, L. Dan, and S. Li, "Improved SLM for PAPR reduction in OFDM system," in *Proc. IEEE PIMRC*, 2007, pp. 1–5.

[54] L. Yang, K. K. Soo, S. Q. Li, and Y. M. Siu, "PAPR reduction using low complexity PTS to construct of OFDM signals without side information," *IEEE Trans. Braoadcast.*, vol. 57, no. 2, pp. 284–290, Jun. 2011.

[55] C. P. Li, S. H. Wang, and C. L. Wang, "Novel low-complexity SLM schemes for PAPR reduction in OFDM systems," *IEEE Trans. Signal Processing*, vol. 58, no. 5, pp. 2916–2922, May. 2010.

[56] E. Al-Dalakta, A. Al-Dweik, A. Hazmi, C. Tsimenidis, and B. Sharif, "PAPR reduction scheme using maximum cross correlation," *IEEE Commun. Lett.,* vol. 16, no. 12, pp. 2032–2035, Dec. 2012.

[57] WiMax solid-state power amplifier SSPA 2.30-2.40-400, CA, USA. [Online]. Available: http://www.aethercomm.com/products/29

[58] K. Bae, C. Shin, and E. J. Powers, "Performance analysis of OFDM systems with selected mapping in the presence of nonlinearity," *IEEE Trans. Wireless Commun.,* vol. 12, no. 5, pp. 2314–2322, May 2013.

초 록

본 논문에서는 직교 주파수 분할 다중화 (OFDM) 방식에 대한 연구를 수행하였다. OFDM 신호의 높은 최대 전력 대 평균 파워비 (PAPR)로 인하여, 이를 낮추기 위한 여러 기법들이 제안되었다. 선택 사상 기법 (SLM), 부분 전송 시퀀스 (PTS), 클리핑, 톤 예약 기법이 소개되었다. PAPR 성능은 우수하지만 여러 번의 역 퓨리에 변환 (IFFT)을 수행하는 데에 따른 SLM 기법의 높은 계산량 때문에, 저복잡도 SLM 기법이 많은 연구가 되었다. 최근에는 PAPR을 낮추기 위해서가 아닌 비트 오류율 (BER)을 개선시키기 위한 기법들이 제안되었다. 상호 변조 왜곡 방식 (IMD), 왜곡 대 신호 전력 비 방식 (DSR), 상관 (correlation) 매트릭 SLM 기법이 그 예이다.

첫째로, 저복잡도 SLM 기법으로 제안된 Class-III SLM 기법의 PAPR 성능을 개선하였다. 기존의 방식은 랜덤하게 순환 이동 값 및 회전 값을 선택하지만, 제안하는 방식은 회전 값의 사용 없이 고정된 순환 이동 값을 이용하여 우수한 PAPR 성능을 얻을 수 있다. 후보 신호들 간의 상관성 (correlation)이 작아지기 위한 최적의 조건을 제안하였으며, 이를 만족시키는 순환 이동 값을 제안하였다. 또한, 회전 값을 이용하여, 최적은 아니지만 우수한 PAPR 감소 성능을 가지는 방식도 제안하였다. 랜덤한 값을 선택하는 방식을 고정된 값을 이용하는 방식으로 변환함에 따라, 부가정보의 양을 줄일 수 있었으며 회전 값에 이용되는 메모리의 크기를 줄일 수 있었다. 또한, 제안하는 방식은 항상 최적의 PAPR 감소 성능을 보장한다.

둘째로, BER 성능을 향상시키기 위한 상관 매트릭을 이용한 SLM 기법의 복잡도를 감소하였다. 일반적으로, 최대 전력을 유추하기 위해서는 4배의 오버샘플링을 이용해야 한다고 알려져 있다. 마찬가지로, 기존의 방식에서 사용되는 상관 매트릭은 4배 오버샘플링을 이용해야 좋은 성능을 얻을 수 있다. 오버샘플링이 된 신호는 Nyquist-rate 샘플들에 의해 표현될 수 있다는 사실을 이용하여, 상관 매트릭의 결과값을 임의의 오버샘플링을 이용한 수식으로 변환하였다. 그에 따라, 임의의 오버샘플

링을 사용했을 때, 얻을 수 있는 상관 매트릭의 결과값을 비교할 수 있었다. 그 결과로, 2배의 오버샘플링을 이용하게 되면 4배 또는 그 이상의 오버샘플링을 사용했을 때와 마찬가지의 BER 성능을 얻을 수 있음을 보였다. 또한, 4배 오버샘플링을 이용했을 때의 선택된 위상 변환 벡터를 2배 오버샘플링을 이용했을 때와 비교한 결과 항상 같은 위상 변환 벡터가 선택된다는 실험 결과를 얻었다. 따라서, 수학적인 분석이 타당하다는 결론을 얻을 수 있었다. 2배의 오버 샘플링을 이용함에 따라, 역 퓨리에 변환의 사이즈가 반으로 줄어들게 되고, 상관 매트릭의 결과 값을 구하는 복잡도도 반으로 줄일 수 있었다

주요어: 비트 오류율 (BER), 상관 (correlation) 매트릭, 선택 사상 기법 (SLM), 직교 주파수 분할 다중화 (OFDM), 최대 전력 대 평균 파워비 (PAPR)
학번: 2011-30965